Cenozoic deformation of the South African plateau, Namibia: Insights from planation surfaces

Carole Picart, Olivier Dauteuil, M. Pickford, François Mvondo Owono

Cenozoic deformation of the South African Plateau, Namibia: insights from planation surfaces

C. Picart[1], O. Dauteuil[1*], M. Pickford[2], F. Mvondo Owono[3]

[1] University of Rennes, CNRS, Géosciences Rennes - UMR 6118, F-35000 Rennes, France

[2] CR2P, MNHN, CNRS, UPMC, Sorbonne University, 38, 57 rue Cuvier, F-75231 Paris cedex 05, France

[3] Department of Earth Sciences, University of Douala, B.P. 2701, Douala, Cameroon

*Corresponding author: Olivier Dauteuil (olivier.dauteuil@univ-rennes1.fr)

Abstract:

Passive margins and associated inland areas display complex vertical displacements that have been abundantly described offshore but much less so onshore due to erosion. Planation surfaces are ubiquitous markers inland that can be used as a proxy both climatic conditions and changes in vertical displacements induced by both short (faults) and long (tilting, flexure) wavelength deformations. We propose 1) a synthetic typology of the planation surfaces driven by a genetic process (weathering versus mechanical erosion), and 2) a method to use these surfaces to map short and long wavelength deformations. This methodology was applied to the Namibian margin and inland plateau to quantify the Cenozoic deformation. The results show that the Namibian margin was affected by bulging during the Oligocene and by an E-W to NW-SE extension during the Late Miocene and Pliocene. The bulge is parallel to the shoreline with a wavelength of 300 km and an amplitude up to 500 m. After investigating the available deformation processes, we propose that an increase in the spreading rate along the mid-oceanic ridge during the Oligocene generated this bulging. The vertical displacement is partially maintained afterwards via isostasy because of mass loss generated by scarp retreat. A minimum average rate of scarp retreat of 5 km/Myr was calculated, which is high compared to the rates estimated in other places in the world. We

ascribe this high value to the prior intense weathering period. Indeed, the alteration largely degraded the bedrock and facilitated the formation of the subsequent scarp. This study also reveals that the high reliefs of the Damara domain existed before the Cenozoic, induced by a reactivation of the Damara structures.

Research highlights

- Bulging affected the South African plateau during the Oligocene.
- Planation surfaces record inland short and long wavelength.
- Eocene weathering event controls the Late Cenozoic of the South African landscape.
- An elevated topography was present before the Paleogene in the Damara domain.

Keywords: morphotectonics, planation surface, bulge, landscape growth, scarp retreat, ridge push

1 Introduction

The post-rift evolution of a passive margin is usually seen as resulting from a subsidence in the offshore domain, driven by thermal cooling and sediment loading, and an uplift of the onshore domain, as a flexural response to lithospheric necking and offshore loading. The flexural response is maintained by the erosion of the tilted blocks and generates scarp retreat inland (Gallagher et al., 1998; Gallagher and Brown, 1999a; Gilchrist and Summerfield, 1991). The relationships between offshore subsidence and onshore uplift are complex (Green et al., 2018) and can be difficult to constrain because offshore and onshore domains are often studied independently. Braun et al. (2013) and Dauteuil et al. (2013b) explored these relationships using numerical modeling, which investigated the flexural behavior of the lithosphere from the oceanic crust to the continental crust. This modeling predicts a long wavelength flexure of around 1000 km in the onshore domain and a shorter one in the offshore domain (hundreds of km). The flexure is at its maximum 10 Myr after the continental breakup and decreases thereafter. After 20 Myr, the flexure disappears and the inland part of the margin is uplifted. This uplift is a dynamic response to unloading generated by erosion. Conversely, the post-breakup deformation is poorly documented onshore because of the lack of pertinent markers recording this deformation. Even in the case of elevated continental margins such as in Scandinavia, Greenland, eastern Australia and southern Africa, various mechanisms are proposed. Onshore displacements are a key component of the evolution of the margin because they drive sediment production and its transfer to the ocean: they can create both sedimentary basins and the relief feeding them (Tinker et al., 2008a; Braun et al., 2013; Rouby et al., 2013). Southern Africa is a case area to study the long wavelength deformation affecting the passive margin and its surrounding area because no orogenic event affected this region after the breakup. We focused our work on Namibia, which is an ancient passive margin that formed 130 Myr ago. The sedimentary archives in the Namibian offshore basins recorded the long-term evolution in three steps (Baby et al., 2018): driven by the flexural response to the continental breakup during the middle Cretaceous, an increase in the sediment supply during the Late Cretaceous, and a low sediment supply during the Cenozoic consecutive to low deformations and a major aridification.

The African topography displays a bimodal distribution of the elevations, while the other continent displays a distribution with an exponential decrease (Dauteuil et al., 2009). This particularity is due to the South African plateau, which covers one quarter of the African surface area. The origin of this plateau is debated. Several hypotheses have assumed a plateau rise, the age of which is still being debated: during the Mesozoic (Nyblade and Sleep, 2003; Pysklywec and Mitrovica, 1999; van der Beek et al., 2002), in the Jurassic, the period of establishment of the Karoo volcanics (Cox, 1989), in the Late Cretaceous (Gallagher and Brown, 1999a, 1999b; Tinker et al., 2008a, 2008b; de Wit, 2007, Baby et al., 2018; Kounov et al., 2008; 2009), or in the late Cenozoic ~ 30 Myr (Burke, 1996; Burke and Gunnell, 2008; Dauteuil et al., 2013a); and ~3 Myr (Partridge and Maud, 1987). Other models suggest that the abnormal elevation of the plateau was inherited from the Triassic, at least (Dauteuil et al., 2013a; Doucoure and de Wit, 2003).

Many previous works (Partridge and Maud, 1987; Gilchrist and Summerfield, 1994; Pysklywec and Mitrovica, 1999; Smith, 1982; van der Beek et al., 2002; Doucoure and de Wit, 2003; Nyblade and Sleep, 2003; Fernàndez et al., 2010; Hirsch et al., 2010) have described uplift or tilting episodes assuming that this deformation is homogeneous at the scale of the plateau. Apatite fission-track analysis distinguishes three cooling phases affecting the plateau and margin: i) from the Silurian to the Permian, ii) from the Jurassic to the Early Cretaceous, and iii) in the Late Cretaceous (Gallagher and Brown, 1999b, 1999a; Raab et al., 2002b; Tinker et al., 2008a, 2008b; Kounov et al., 2013; Braun et al., 2014). The first cooling stage documents the erosion associated with the planation of the Damara orogeny. The

Jurassic to Early Cretaceous stage is associated with the Karoo and Etendeka magmatic events and rifting (Wildman et al., 2016). The increase in the Late Cretaceous denudation is driven by an uplift of the plateau generated either by the reorganization of the plate kinematics (Raab et al., 2002b) or by the installation of a superswell under the plateau (Braun et al., 2014). These studies assume the global uplift of the entire plateau, except for Raab et al. (2002b), who proposed a differential uplift between the northern and southern parts of Namibia. Because of the limitations of this method, these studies did not detect low deformation, which can affect the plateau. However, some studies have described i) localized deformations during the Cenozoic, for instance, in the Fish River Canyon (Mvondo et al., 2011), to the north of the Orange River (Goudie, 2005; Dauteuil et al., 2015; Dauteuil et al., 2018) or in the Okavango Rift system (Pastier et al., 2017), and ii) long wavelength deformation influencing the landscape evolution (Haddon and McCarthy, 2005; Goudie, 2005; Dauteuil et al., 2013a, 2013b; Wildman et al., 2016). In this paper, we quantify the short and long wavelength deformations that affected the Namibian plateau during the Cenozoic, by considering the associated margin. The work is based on a detailed geomorphic analysis because this domain has been subjected to erosion and weathering since the mid-Cretaceous.

2 Geological and geomorphic setting

Namibia can be classified into three geomorphic domains: a low-relief coastal plain to the west, an elevated inner plateau in the middle part and a high relief dissected area to the north and between the inner plateau and coastal plain (Fig. 1). The coastal domain, including the Sperrgebiet, extends from the present-day shoreline to the scarp at an elevation of ca. 800 m. This domain is largely etched with remnant hills mainly located close to the scarp. The inner plateau has a mean elevation of 900 m with summits up 2200 m and displays several vast planation surfaces limited by an erosional scarp and incised by several rivers (Dauteuil et al., 2015; Mvondo Owono et al., 2016). Parrish et al. (1982), Burke and Gunnel (2008), Pickford et al. (2014) and Guillocheau et al. (2018) have described climate changes in southern Africa during the Cenozoic. After a humid period at the end of the Cretaceous, the climate became hot and dry during the Paleocene. Then the Paleocene-Eocene Thermal Maximum (PETM) occurred, and the climatic conditions evolved to hot and humid during the Eocene and generated thick lateritic profiles (see the synthesis in Miller et al., 2008). During the Oligocene, the temperature and rainfall decreased. During the Miocene, aridification started following the installation of the Benguela current during a phase of Antarctic ice sheet growth. The aridity has increased since the Pliocene as a consequence of the first glaciation (Dupont et al., 2005; Jung et al., 2014).

Cratons and mobile belts of Archean and Precambrian age structured the basement of the South African plateau. During the Neo-Proterozoic, the genesis of the Damara Belt and Gariep Belt, deformed the Namaqualand Metamorphic Complex (Bumby and Guiraud, 2005; Kounov et al., 2013) (Fig. 2a). During the Early Cambrian, these two belts confined the Nama Basin in which sediments accumulated from the surrounding mountain ranges (Gresse and Germs, 1993). At the end of the Carboniferous, deposition took place inside a foreland basin due to orogenic loading and produced the Karoo sequence (Bumby and Guiraud, 2005; Stollhofen et al., 1998, Zerfass et al., 2005). During this period, a vast ice sheet covered the entire region and produced the glacial deposits of the Dwyka Formation (Miller et al., 2008) and the lacustrine sediments of the Prince Albert Formation during the deglaciation. At 180 Myr, the eruption of the Karoo basalts (Fig. 2d) marked the initiation of the continental breakup of Western Gondwana (Jourdan et al., 2005; Miller et al., 2008). The opening of the Atlantic Ocean during the Barremian corresponds to the last major geodynamic event (Aslanian et al., 2009; Moulin, 2003; Olivet et al., 1984) and is associated with the Etendeka-Parana magmatic event (Marsh and Milner, 2007; Owen-Smith et al., 2017). Since then, erosion and weathering have largely affected the Namibian plateau (Burke and Gunnell, 2008; Pickford and Senut, 1999b). An intense weathering phase occurred during the Paleocene and Eocene: it largely affected the basement rocks generating a thick lateritic profile (Fig. 2b, 2e) (Pickford and Senut, 1999b; Mvondo Owono et al., 2016; Guillocheau et al., 2018). Cenozoic deposits are scarce over the Namibian plateau. The Kalahari Formation, along with fluvial and aeolian deposits, accumulated on top of the Early Mesozoic to Proterozoic units during the Miocene (Haddon and McCarthy, 2005; Linol et al., 2014; Wanke and Wanke, 2007). The inner domain is also characterized by calcrete, which forms a tabular upper layer (1-2 m thick) over a wide area (Pickford, 2016). The age of the calcrete is debated: Late Miocene (Goudie & Viles, 2015; Ward, 1987) or Plio-Pleistocene (Pickford et al., 1999a). On the coastal plain, the aeolian dunes in the Namib Desert have covered the basement since the late Early Miocene. The Sperrgebiet displays Tertiary to Quaternary deposits in various depositional environments: marine, palustral, fluvial, deltaic and aeolian (Miller et al., 2008;

Pickford, 2016; Pickford and Senut, 2003). The marine event lasted from the middle Eocene to the lower Oligocene (Pickford and Senut, 2003; Miller et al., 2008; Pickford, 2016). Then, fluvial deposits track large rivers that are more or less perpendicular to the present-day shoreline, active from the middle Oligocene to the Burdigalian (Pickford, 2016). Since the middle Neogene, scarce deposits are associated with the aridification of south-west Africa. The Cenozoic history is also characterized by magmatic events both on the coastal plain and inland. They correspond to phonolites (Klinghardt - 46 Ma; Marsh, 2010), the Staalhart and Aris massifs - 46 to 52 Ma (Lock, 1973; Fig 2c), Kimberlites (Gibeon province; Nguno, 2004) and carbonatites (Dicker Willem massif - 49 Ma; Cooper, 1988) and the Gross Brukkaros massif - 75 Ma (Lorenz et al., 2000).

3 Methodology and data

The Meso-Cenozoic deformation was investigated by using two kinds of markers: the planation surfaces and the unconformity between the Nama Formation of Neo-Proterozoic age and the Namaqualand Metamorphic Complex of Meso-Proterozoic age. These two markers cover large geographic areas (several hundreds of kilometers) within the study area. The unconformity between the Nama Formation and the Namaqualand Metamorphic Complex is a large planation surface that seals the Meso-Proterozoic orogenic cycle. This erosion surface is assumed to be horizontal when formed and poorly affected by a later orogeny, especially in the middle domain of the southern plateau. The glacial deposits of the Karoo sequence remain parallel to this unconformity confirming this hypothesis. We used this unconformity because of its large geographical extent.

3.1 Planation surfaces

The inner parts of continents are largely shaped by planation surfaces; the genesis of these surfaces have generated numerous debates between geomorphologists for more than a century. Recent works (Guillocheau et al., 2014; Bessin et al., 2015; Dauteuil et al., 2015) have revised the terminology and characterization of planation surfaces: it is based on the processes that form them rather than on the surface geometry, as has been done previously (Partridge and Maud, 2000). Three types of surfaces shaping the continental inland were defined (Table 1): peneplain, pediplain and stripped etchplain. These surfaces provided two kinds of information: climatic changes and variations in the base level. The climatic conditions drive the erosion/weathering process and, as a consequence, the type of surface

(Table 1). The main parameter is the type of rainfall (Mvondo Owono et al., 2016; Guillocheau et al., 2018). In arid conditions, the precipitation is infrequent but intense, so it is efficient in terms of erosion and transport. By consequence, a significant amount of material is transported episodically over long distances by both rivers and floods. This process is dominant in the genesis of pediplains. Very humid periods accentuate the flow of water in permanent rivers, thereby increasing the efficiency of the erosion and leading to the genesis of peneplains. Hot and humid periods allow the genesis of thick soil that is rich in organic matter, which increases the acidity of the groundwater. These specific physical and chemical conditions allow the weathering of the basement, irrespective of its lithology, and generate lateritic profiles.

After climatic conditions, the second process impacting planation surfaces is the variation in the base level induced by either tectonics or sea level changes (Bonow et al., 2006). Variations in sea level are well recorded close to the shoreline and their influence decreases inland because regressive erosion takes time to propagate. In terms of deformation, two cases should be distinguished: short wavelength deformation (faults - Fig. 3a) and long wavelength deformation (flexure, tilting, bending - Fig. 3b). Four types of relationships between faults and planation surfaces occurred (Fig. 3a). The obvious setup corresponds to a fault that offsets a pre-existing surface and generates a scarp. However, a scarp is not always symptomatic of a recent fault: it can also result from differential erosion between two lithological units. As illustrated in Figure 3a, a deeper marker is needed in order to determine whether a fault is present. In this study, we used the unconformity between the Nama deposits and the Namaqualand Metamorphic Complex as a marker.

Long wavelength deformations modify the relative base level that controls the elevation of the planation surfaces (Fig. 3b). The base level corresponds to the sea if the surface is close to the coast (hundreds of km) and is simply connected to it. In this case, a base level fall can be the result of a change in the sea level or uplift. Inland, the base level can be a lake or a major permanent river draining a huge region. A base level fall generates imbricated surfaces with the upper surface being the older surface. Figure 4b illustrates how different large-scale (> 10 km) processes (uplift, tilting and bending) can modify the surface geometry. The planation surfaces display gentle slopes (< 1°) over large areas, thus the elevation distribution is much smaller. A tiny deformation will modify the surface slope and widens the elevation distribution (Fig. 3b). The widening of the distribution is directly relative to the amount of tilting or bending: the higher the deformation the greater the widening. Thus, the elevation distribution is a pertinent proxy for detecting a long wavelength deformation affecting a planation surface.

Planation surfaces were mapped with GIS software using DEM (STRM 30), satellite images (SPOT) and observations made during field trips. Surface heights (Fig. 4) were mapped and their main characteristics are summarized in Table 2.

The major challenge for constraining the landscape growth is the dating of the planation surfaces (Watchman and Twidale, 2002). The difficulties are due to the fact that the planation surfaces evolve permanently with the rate depending on the lithology, local slope and climate. By consequence, the genesis of a planation surface cannot be strictly contemporaneous over its entire extent. It is more convenient to propose a period of formation rather than an age. We used the relative position of each surface (the higher surface being the older one) and the geometric relationships between the surfaces and some well-dated markers such as magmatic events and deposits. The geometrical relationships between the intrusive rocks and the geomorphic markers can be used to propose a period of planation (Parrish et al., 1982; Burke and Gunnell, 2008; Guillocheau et al., 2018). If the magmatic massif intrudes the planation surface and covers it, the planation surface existed before the magmatic event, i.e. is older. If the planation surface was extinguished on the eroded magmatic massif, the planation was active after the magmatic event (Fig. 4).

3.2 Nama-Namaqualand unconformity

The mapping of the planation surfaces alone is not sufficient to determine the deformation features: another marker at depth is required to eliminate erosional scarp (Fig. 3). We chose the unconformity between the Nama Formation and the Namaqualand Metamorphic Complex because it can be mapped throughout the area using outcrops, scarce boreholes and published studies (Stanistreet and Charlesworth, 2001; Blanco et al., 2011). This discontinuity corresponds to a main planation event at the end of the Meso-Proterozoic, which generated a flat and horizontal topography in the middle domain of the Namibian plateau covered by the marine deposits of the Nama Formation (Blanco et al., 2011). The Nama Basin extends from south of the Damara Belt to north of the Orange River. We created an elevation map of the unconformity (Fig. 6) by interpolating the elevation of the unconformity outcrops and depth estimated from geological cross-sections (Fig. 7) (Geach et al., 2014).

4 Landscape shaping

Four domains can be identified when all of the data are integrated: the Damara domain, the inner part, the coastal plain, and the Orange area (Fig. 5). Eight planation surfaces shape the landscape of the study area. A detailed description is given in Table 2.

4.1 The Damara domain

This domain corresponds to the mountain range extending from Windhoek to Walvis Bay and from Usakos to Kalkrand where the Damara Belt predominantly crops out. Six surfaces (S0, S1, S2, S3, S6 and S8) shape this domain, the elevations of which range from 0 to 2500 m. The highest surface (S0) corresponds to a degraded surface topping some elongated NE-SW summits (from 2000 to 2300 m) and passing above the other summits. Surface S1, located to the south and east of Windhoek, has a sinuous shape with mean slope of 0.2° and the elevation ranges from 1450 m to 1900 m. It corresponds to a peneplain dissected by later erosion with an old drainage flowing towards the southeast while the recent drainage flows westwards. Surface S2, located to the north and west of Windhoek, corresponds to wide and long pediplains with elevations ranging from 1300 m to 1650 m. The drainage flows towards the southwest. Surface S3, to the south and east of Windhoek, is associated with inselbergs (Fig. 2b) and stripped laterite profiles (Fig. 2b, 2e). Its elevations range from 1850 m to 1240 m with a regional slope to the southeast. Surface S6, in the north of the Damara domain, is the lowest of the main surfaces shaping this domain. The elevations never reach sea level: they range between 25 m and 1000 m, with a regional slope up to 0.26°. Surface S6 corresponds to a wide pediplain with a slope dipping westwards. Surface S8 corresponds to pedivalleys with present-day rivers flowing seaward that incise surfaces S6 and S7. Some residual hills corresponding to surface S2 remain. Surface S6 forms the floor of the Windhoek graben. Thus, this graben was formed after surface S2 and before surface S6. The drainage associated with surfaces S0, S1, S2 and S3, is roughly oriented southwards indicating a base level located to the south. In the Damara domain, the Nama-Namaqualand unconformity could not be mapped because the geographical extent of the Nama Basin stopped at the southern boundary of this domain. The presence of many imbricated surfaces reveals several successive falls in the relative base level and the progressive slope increase in the planation surfaces, is interpreted as an uplift of this domain. The presence of high residual surfaces (S0, S1, S2) reworked by surface S3 indicates that the elevated topography of the Damara domain existed before the genesis of surface S3 and is therefore old.

4.2. The inner domain.

This domain occupies a wide area located entirely in the elevated plateau from south of Rehoboth to south of Keetmanshoop. This area is shaped by four stepped planation surfaces (S3, S4, S5 and S6). They are elongated in a N-S direction dipping southwards. The elevation step between each surface is up to 250 m revealing a significant base level fall. Surface S3 is clearly recognizable in the landscape because it retains numerous inselbergs and was used as a geomorphic marker. Surfaces S4 and S5 largely cover the central part and mainly affect the sediments of the Nama Group. They display a drainage network configured by N-S oriented streams (Konkiep River and Fish River) with short E-W tributaries mainly located on the western side of the associated plain. The eastern N-S (Fig. 7a) cross-section displays a bending of the surface slopes to the south of Gibeon, interpreted as a slight southward bending of the southern part of this domain. The E-W cross-sections show the highest slopes for the planation surfaces on the western border, which is interpreted as an uplift of this western border.

The unconformity between the Nama unit and the Namaqualand Metamorphic Complex displays a large depression (200 km x 200 km at least) with a flat bottom at an elevation close to 0 m and elevated borders up to 2000 m to the west and up to 1800 m to the north. The flatness of the central part is partially due to the scarcity of data under the Kalahari where the elevation was estimated from geological cross-sections and boreholes.

4.3 The coastal domain

The coastal plain is a wide, heavily eroded domain with elevations ranging from 0 to 950 m, and which is limited to the west by the main scarp. The planation surfaces are difficult to map continuously because of dune fields, which cover more than half of this domain. Many of the remnant hills are close to the scarp and often comprise inselbergs. Four surfaces shape this domain: S3, S6, S7 and S8, which can be gathered into two sets. The high surface, S3, is very degraded and only crops out at a few remnant hills that are inselbergs. Some stripped lateritic profiles located in the Sperrgebiet confirm that a major weathering event also affected this coastal domain. The unconformity crops out in small places mainly in the Sperrgebiet.

Thus, the erosion that generated the main scarp occurred between surfaces S3 and S6 and corresponds to a major fall in the base level. Surface S7 is on the shoreline side of the coastal domain. The slope break separates it from surface S6: surface S7 is steeper than surface S6 (Fig. 7b). It reworks surface S6 and has elevations ranging from sea level to 300 m. The last and youngest surface is S8, which forms a very narrow band on the shoreline and enters the coastal, Damara and Orange domains along recent rivers.

4.4 The Orange domain

The landscape in this area displays five planation surfaces. The two older surfaces (S3 and S4) are very degraded and S5 is partially degraded, while the two younger surfaces (S6 and S8) are well-preserved. Surface S6 displays a dendritic drainage that slightly incises the topography and flows eastward to southward while the drainage on surface S8 trends southwestward to westward. This domain is largely affected by faults that offset surfaces S3, S4 and S6, as in the Fish River Canyon and the Karas mountains (Fig. 5, southern section in Fig. 7b). These faults mostly trend N-S, although some of them are oriented NE-SE and NW-SE. They have a vertical throw up to 250 m. In the Karas mountains, they generate a set of horsts and grabens confined to a band trending ENE-WSW from the east of Rosh Pinah to the south of Keetmanshoop. The unconformity crops out widely. It displays an undulating shape with a 200-km-long wavelength and an amplitude of 500 m (Fig. 7b). It is offset by the fault system. Surface S4 and the more recent ones are also affected by the long 200 km wavelength, which is not observed in the inner and Damara domains. The unconformity is a major planation surface covered by marine deposits and was horizontal when it was overlain. As a consequence, the wavelength was acquired after its genesis and after the genesis of surface S4.

5 Age of the planation events

Figure 8 summarizes the various dated markers used to constrain the age of the planation surfaces. In the Sperrgebiet, some Meso-Cenozoic continental deposits tens of meters thick fill valleys connected to the sea (Miller et al., 2008; Pickford, 2016) (Fig. 5). These Mio-Pliocene deposits overlie surface S8. The sand field of the middle Miocene Namib desert covered surface S6 indicating that this surface is older than the middle Miocene. To the east of the town of Mariental, an alluvial delta deposited above the weathered Karoo basalts crops out (Fig. 8). From bottom to top, the delta is formed of shales, conglomerates with basaltic clasts, fine sandstone with basaltic clasts, debris flow, calcified mudflow, conglomerates with sandy cement and medium sandstone. Calcrete, measuring 1-2 m thick, tops the delta deposit: it corresponds to the Kalahari calcrete of late Miocene or Plio-Pleistocene age (Miller et al., 2008). The current features indicate a flow from the south. This deltaic sequence was deposited on the surface truncating the weathered basalts: surface S3. Surface S5 erodes the delta deposits, the Karoo basalts and the Dwyka Formation. The upper surface of the delta was eroded flat before the formation of the calcrete and corresponds to an intermediate planation surface, i.e. surface S4. The difference in elevation between surfaces S4 and S5 is 50 m, which corresponds to major erosion following a base level fall. The timing of the delta deposits is constrained by these two surfaces: it started after the Eocene weathering period and could have been deposited during the Upper Eocene (Parrish et al., 1982; Pickford et al*.*, 2014; Guillocheau et al., 2018). As a consequence, surface S4 was generated during the late Eocene, and surface S5 during the early Oligocene. Surface S3 is an etchplain that cut the Dicker Willem complex and the Rehoboth phonolites, which were both weathered. Thus, surface S3 was generated during the middle Eocene. Surfaces S0, S1 and S2 are older than S3, i.e. older than the Eocene, and are younger than the middle Jurassic because they completely eroded the Etjo Sandstone Formation to the north of the Damara domain. They mainly affect the Damara schists, the lithology of which is not favorable for the development of thick lateritic profiles. Thus, no ages were suggested for these three surfaces S0, S1, S2.

6 Deformations

The map of the planation surfaces (Fig. 5) was combined with the map of the unconformity depth (Fig. 6) in order to map the deformation field including both faulting and medium-to-long wavelength deformations. As presented in section 3, the faults were mapped from the offsets of the planation surfaces and unconformity; the medium-to-long wavelength deformation was determined from the stepping of the surfaces, the change in slope and the shape of the unconformity.

Three sets of faults, trending NE-SW, N-S and NW-SE, affected the study area. Their throws are mainly vertical, from tens to hundreds of meters. Most of them are located in an E-W corridor located to the north of the Orange River and form a set of horsts and grabens

(Mvondo et al., 2011). Their orientation displays a divergent organization with a NE-SW direction to the east, a N-S direction in the middle part and a NW-SE orientation to the west (Fig. 5), as described on geological maps (Genis, 1990; Schreiber and Becker, 1999). Some scarce NW-SE faults affect the central domain and coastal plain, such as the Hebron Fault that offsets surface S6 (White et al., 2009). N-S normal faults affected the Damara domain generating the two grabens in the area of Windhoek that offset surface S2. Fracturing deformed surface S5, providing an age that is younger than the late Oligocene for this extensive deformation.

The planation surfaces are organized into three groups: the surfaces of the first group (S3 and S4) are mainly located in the inner plateau, the surfaces (S5 and S6) of the second group are both inland and in the coastal domain, and the surfaces (S7 and S8) of the third group are in the coastal domain. The difference in elevations is greater between the first and second groups (up to 500 m) than between the second and third groups (up to 20 m), as illustrated in the western profile in Figure 6a for instance. The planation processes tend to equilibrate the topography to the base level. As a consequence, stepped planation surfaces reveal a change in the base level, which is due either to a sea level variation or deformation. The difference in elevation (20 m) between the second and third groups, the location of surfaces S7 and S8 (mainly in the coastal domain) and the lack of known faults and an uplift proxy such as river knick points indicate that their stepping was largely driven by the variations in sea level. The stepping of the surfaces between the first and second groups (up to 500 m) are compatible with a base level fall induced by tectonics because the steeping up to 500 m is greater than the sea level variations (< 200 m). The map shown in Figure 10 illustrates the differences in elevation between S3 and S6, as they are the most representative and most ubiquitous surfaces. For each surface, its geometry was estimated from an interpolation of the present elevation of the outcrops of the surface. This map illustrates the local eroded volume that is driven both by climate and the local slope. Assuming a homogeneous climate at the scale of the plateau for a given time, this local increase in erosion is attributed to an increase in the local slopes induced by a deformation. These changes in slopes occur on both sides of an elongated N-S shape that has a 300 km wavelength in a domain that is roughly parallel to the coast, from latitude 22°S to latitude 26°S. A second area with a major increase in slope is located around the Fish River Canyon, which is largely affected by the previously described faults. The deformation pattern strongly suggests a bulging at the regional scale between the genesis of the S3 and S6 surfaces, i.e. mainly during the Oligocene.

7 Discussion

This geomorphic study highlights how deformation and climate drive landscape evolution. The process that generated the planation surfaces provides constraints on i) the climate, which controls the relative contribution of mechanical erosion versus chemical weathering, and ii) the tectonics, which controls the shape and the spatial relationships between the different surfaces. Although fault mapping based on geomorphic markers is commonly done, we present a method that can be used to quantify the regional bulging and bending occurring in the erosional domain. This geomorphic method provides an integrated overview of the deformation occurring in an area regardless of the wavelength, and as a result, we can have access to both crustal and mantle dynamics. The landscape evolution of the Namibian plateau resulted in a succession of nested planation phases. Several processes can generate such organization. The first parameter to consider is the lithology. All of the lithologies (metamorphic basement, intrusive massifs, sediments and basalts, etc.) were affected by planation, whatever their internal structure (strata or foliation). A given surface cuts across several lithologies. Only surface S5 is parallel to the stratification interface between two inner units of the Nama sequence. This result confirms a detailed study done in the Orange River domain (Dauteuil et al., 2015) and the regional study of Mvondo Owono et al. (2016), which points out that there is no relationship between lithologies and planation, as the lithology only has an impact on a small scale: there are no fits between the lithology map and surface map.

7.1 Namibian landscape evolution

The spatial distribution of the planation surfaces is in agreement with the ages provided by the Apatite fission-track analysis (AFTA) (Gallagher and Brown, 1999a; Brown et al., 2002; Raab et al., 2002b; Luft et al., 2005; Tinker et al., 2008a, 2008b; Kounov et al., 2013). The AFTA ages younger than 90 Ma are located in the coastal plain and on both sides of the Orange River: they are associated with the youngest and lowest surfaces (S6, S7 and S8). In contrast, the oldest AFTA ages (> 350 Ma) are located in the Damara domain, which displays numerous elevated planation surfaces indicating an old geomorphic history. In the central domain, the AFTA ages range from 100 Ma to 200 Ma, corresponding to intermediate surfaces that were slightly reworked afterwards. The Damara domain without well-developed planation surfaces displays ages as young as the Cenozoic and the modelling of the thermal evolution of samples with ages younger than 130 Ma suggest Cenozoic deformation (Luft et al., 2005; Brown et al., 2014; Fairhead and Binks, 1991; Raab, 2002a).

Numerous inselbergs shape the S3 etchplain: they result in the etching of the weathering profiles. Many of them are higher than 100 m, up to 250 m: they reveal very deep weathering, much greater than the classic thickness of the lateritic profiles: from 50 m to 90 m (Boulangé and Millot, 1988; Butt et al., 2000). The thickness of the weathering profile is driven by the depth of the deep aquifer that controls the water flow to avoid chemical saturation (Tardy, 1993). Two hypotheses can generate deep weathering. A first model suggests that a very thick profile is induced by a lowering of the water table and/or an increase in humidity (Butt et al., 2000). The second model proposes a polyphase evolution with a succession of weathering periods followed by erosive periods. Data on the paleoclimatic conditions in the study area are scarce for the Eocene period. No changes in the climate conditions have been described. In addition, the most efficient process for lowering the water table is vertical displacement: the base of the lateritic profile becomes shallower than the water table, which increases the water flow (Tardy, 1993). Thus, the upward displacement of the Namibia plateau started during the main period of weathering and could represent the preliminary stage of Eocene bulging.

The evolution of the Cenozoic landscape (Fig. 11) principally derived from the weathering phase that occurred during the Eocene (Pickford and Senut, 1999b). This weathering affected the preexisting high Damara domain, north of the study area, as attested by the presence of elevated inselbergs. Therefore, the Damara relief existed before the Early Cenozoic as attested by the presence of surface S3, which is contemporaneous to the weathering period. A presence of elevated relief during the Late Cretaceous was proposed by Raab et al. (2002b) who point out a reactivation of preexisting structures, confirming our hypothesis regarding the age of this relief. During the Eocene, the weathering deeply affected the entire region by developing thick lateritic profiles (> 100 m) (Mvondo Owono et al., 2016) that were dismantled by mechanical erosion after a change in the climate from humid to semi-arid. This change generated wide pediplains. The second main event that modified the planation process is the Oligocene bulging. It lowered the base level, which increased mechanical erosion and generated two stepped pediplains (S5 and S6). The youngest surfaces (S6, S8) located in the inner domain are not affected by bulging.

The presence of planation surfaces on the coastal domain allows the recovery of the period during which the escarpment was retreating: it occurred between the formation of surface S3 (middle Eocene) and surface S6 (early Miocene). The difference in elevation between these surfaces is up to 500 m. The planation surfaces reveal that the coastal plain generated by the scarp retreat started in the early Miocene and lasted until today, i.e. over 20 Myr. Assuming reasonably that the shoreline was close to the present-day position, the minimum scarp retreat is 100 km, and up to 150 km. Thus, the average rate of scarp retreat ranges from 5 km/Myr to 7.5 km/Myr. Cockburn et al. (1999) estimated a rate less than 1 km/Myr assuming that the scarp retreat started at the end of the rifting, i.e. 130 Myr. However, this late age is not consistent with the etching of the Dicker Willem intrusion, located in the coastal plain, which occurred after its emplacement during the lower Eocene. The scarp retreat rate estimated in this study corresponds to a high rate compared to the other rates: 0.1 km/Myr for the Drakensberg Escarpment (Fleming et al., 1999), 0.5 to 6.7 km/Myr in the Colorado plateau (Schmidt, 1989), 2 km/Myr for the Australian Great Escarpment, 6 km/Myr in the Gulf of Suez (Steckler and Omar, 1994) and 2-3 km/Myr at the western Indian coast (Gunnell and Fleitout, 1998). The cosmogenic analysis indicates a denudation rate that is lower by several orders of magnitude (> 20 m/Myr) (Bierman et al., 2014; Cockburn et al., 1999; Kounov et al., 2007). These very low rates were estimated for recent periods (Pliocene or younger). The rapid scarp retreat associated with the high denudation rate estimated in this work resulted from a combination of the high efficiency of mechanical erosion following the previous weathering phase, which deeply degraded the bedrock, and a humid period that transported material to the sea. The low values estimated for recent periods result both in the unfavorable climatic conditions (arid to semi-arid) and in the lack of degraded material that was previously evacuated.

7.2 Deformation process involved

The deformation analysis points out that the Namibian plateau and coastal plain were affected by two deformations during the Cenozoic: a N-S bulging and an intense faulting mainly located to the south. The generated bulge has a 300 km wavelength in the central part and disappears towards the south. This long wavelength implies a process at the lithospheric scale. It is interesting to note that this bulging started when the sea level was in an upward trend (Miller et al., 2011). This corresponds to the abandonment of the marine flooding surface (S7) and to the beginning of the terrigeneous deposits in Sperrgebiet.

Several mechanisms generate this flexural deformation at the lithospheric scale (Salomon et al., 2015). The process classically involved in a context of a passive margin is a flexural response to lithospheric thinning affecting an elastic plate (Braun and Beaumont, 1989). The numerical simulations of Braun et al. (2013) showed that an inland bulging occurs mainly 10 to 20 Myr after the continental breakup, and affects the inland part over a distance of 600 km. After the maximum of uplift that lasted 10 Myr, the upward displacement becomes homogeneous over the entire continent and decreases progressively with time. However, this process cannot be proposed for the Namibian landscape because the bulging described in this study occurred more than 100 Myr after the continental breakup. The second possible model is the dynamic topography in which part of the topography results from the dynamic support from the sublithospheric mantle caused by low-density mantle anomalies and/or stresses generated by mantle flow. This hypothesis was proposed to explain abnormal elevations such as those found in Scandinavia, southern Africa (Artemieva and Vinnik, 2016; Flament et al., 2014; Forte et al., 2011; Simmons et al., 2009) or eastern Australia (Rovere et al., 2014). In southern Africa, the amplitude of the dynamic topography is controversial: from several tens of meters (Forte et al., 2011) to more than one kilometer (Flament et al., 2014). The expected wavelength is thousands of kilometers and the maximum uplift occurred 50 Myr ago (Flament et al., 2014). Our study points out that a bulging phase occurred 25 Myr ago, up to 500 m high for a wavelength of some hundreds of kilometers (< 500 km): the timing, amplitude and wavelength are not compatible with the dynamic topography model. The third process producing upward displacements is the migration of the African Plate over of a mantle plume during the Turonian (Braun et al., 2014). This migration may have impacted the continent for as long as 20 Myr, i.e. until the early Paleocene. However, this process is also too early to explain an Oligocene bulging. The last mechanism is a change in the push induced by the mid-oceanic ridge, which has often been proposed to explain compressive features observed on passive margins (Bott, 1973; Japsen et al., 2012; Le Breton et al., 2012). Two types of driving forces act: the volume forces induced by the differences in the bathymetry and the thickness of the oceanic lithosphere between the oceanic ridge and the ocean-continent boundary, and the temporal and spatial variations in plate motion. The process of the ridge push reactivates preexisting features that should be submit to an horizontal compression (Leroy et al., 2004). The data for the half-spreading rates (Cande et al., 1988; Müller et al., 2008) display an increase in the spreading rates from the late Eocene to the early Miocene with the maximum occurring during the late Oligocene, i.e. contemporaneous with the bulging. This change in rate increases the horizontal compressive stress applied to both the margin and inland thereby generating the bulge. During the middle Miocene, the spreading rate decreased and the diffuse deformation affected the plateau generating more extensive structures (Dauteuil et al., 2018). Therefore, we propose that the upper Cenozoic deformation of the Namibian plateau resulted from two successive processes. Variations in the spreading rate at the end of the Eocene generated the bulging of the coastal domain. The steepening of the slopes increased erosion and the retreat of the scarp. The mass loss was compensated by isostasy which maintained the upward motion and propagated it slightly inland.

8 Conclusions

The deformation of the inner domain of a continent is driven by both deep asthenospheric processes and lithospheric boundary conditions. However, the deformation can be difficult to determine because it is low and the inland domain is heavily eroded. Planation surfaces are the markers that record this deformation. We propose to use them to constrain both the deformation and the landscape evolution. They provide two pertinent constraints: i) climatic conditions, and ii) vertical displacements whatever the wavelength. Although a short wavelength deformation (fault) is easy to map, a long wavelength deformation can only be determined from these geomorphic proxies.

Using this method, we highlight that the Namibian margin and associated plateau were affected by a bulging with a wavelength of 300 km of during the Oligocene. It occurred 100 Myr after the continental breakup and thus could not be ascribed to this breakup. This bulging is contemporaneous with an increase in the spreading rate of the mid-Atlantic ridge. The erosion of the bulge generated the present-day escarpment with a rate of scarp retreat from 5 to 7.5 km/Myr. We ascribe this high value to the Paleocene weathering period, which deeply degraded the bedrock and drove the landscape evolution during the Cenozoic. The geomorphic evolution proposed in this study constitutes a reference for further studies on the source-to-sink balance between onshore and offshore domains.

Acknowledgements

The CNRS-INSU project Action Marges funded this work. We thank P. Bessin and P. Japsen for useful and constructive discussions. The field trip in Sperrgebiet (Namibia) was organized with the authorization of the Namdeb Diamond Corporation in Lüderitz.

References

Artemieva, I.M., Vinnik, L.P., 2016. Density structure of the cratonic mantle in southern Africa: 1. Implications for dynamic topography. Gondwana Res. 39, 204–216. https://doi.org/10.1016/j.gr.2016.03.002

Aslanian, D., Moulin, M., Olivet, J.-L., Unternehr, P., Matias, L., Bache, F., Rabineau, M., Nouzé, H., Klingelheofer, F., Contrucci, I., Labails, C., 2009. Brazilian and African passive margins of the Central Segment of the South Atlantic Ocean: Kinematic constraints. Tectonophysics 468, 98–112.

Baby, G., Guillocheau, F., Morin, J., Ressouche, J., Robin, C., Broucke, O., Dall'Asta, M., 2018. Post-rift stratigraphic evolution of the Atlantic margin of Namibia and South Africa: Implications for the vertical movements of the margin and the uplift history of the South African Plateau. Mar. Pet. Geol. 97, 169–191. https://doi.org/10.1016/j.marpetgeo.2018.06.030

Bessin, P., Guillocheau, F., Robin, C., Schroëtter, J.-M., Bauer, H., 2015. Planation surfaces of the Armorican Massif (western France):Denudation chronology of a Mesozoic land surface twice exhumed in response to relative crustal movements between Iberia and Eurasia. Geomorphology, Patterns and rates of Cenozoic landscape change in orogenic and post-orogenic settings 233, 75–91. https://doi.org/10.1016/j.geomorph.2014.09.026

Bierman, P.R., Coppersmith, R., Hanson, K., Neveling, J., Portenga, E.W., Rood, D.H., 2014. A cosmogenic view of erosion, relief generation, and the age of faulting in southern Africa. GSA Today 24, 4–11. https://doi.org/10.1130/GSATG206A.1

Blanco, G., Germs, G.J.B., Rajesh, H.M., Chemale Jr., F., Dussin, I.A., Justino, D., 2011. Provenance and paleogeography of the Nama Group (Ediacaran to early Palaeozoic, Namibia): Petrography, geochemistry and U–Pb detrital zircon geochronology. Precambrian Res. 187, 15–32. https://doi.org/10.1016/j.precamres.2011.02.002

Bonow, J.M., Lidmar-Bergström, K., Japsen, P., 2006. Palaeosurfaces in central West

Greenland as reference for identification of tectonic movements and estimation of erosion. Glob. Planet. Change 50, 161–183. https://doi.org/10.1016/j.gloplacha.2005.12.011

Bott, M.H.P., 1973. Implications of coninental drift to the Earth Sciences, in: Tarling, D.H., Runcorn, S.K. (Eds.), Shelf Subisdence in Relation to the Evolution of Young Continental Margins. Academic Press, London, pp. 675–683.

Boulangé, B., Millot, G., 1988. La distribution des bauxites sur le craton ouest-africain. Sci. Géologiques Bull. Strasbg. 41, 113–121.

Braun, J., Beaumont, C., 1989. A physical explanation of the relation between flanks uplifts and the breakup unconformity at rifted continental margin. Geology 17, 760–764.

Braun, J., Deschamps, F., Rouby, D., Dauteuil, O., 2013. Flexure of the lithosphere and the geodynamical evolution of non-cylindrical rifted passive margins: Results from a numerical model incorporating variable elastic thickness, surface processes and 3D thermal subsidence. Tectonohysics 604, 72–82.

Braun, J., Guillocheau, F., Robin, C., Baby, G., Jelsma, H., 2014. Rapid erosion of the Southern African Plateau as it climbs over a mantle superswell. J. Geophys. Res. Solid Earth 119, 2014JB010998. https://doi.org/10.1002/2014JB010998

Brown, R., Summerfield, M., Gleadow, A., Gallagher, K., Carter, A., Beucher, R., Wildman, M., 2014. Intracontinental deformation in southern Africa during the Late Cretaceous. J. Afr. Earth Sci. 100, 20–41. https://doi.org/10.1016/j.jafrearsci.2014.05.014

Brown, R.W., Summerfield, M.A., Gleadow, A.J.W., 2002. Denudation history along a transect across the Drakensberg Escarpment of southern Africa derived from apatite fission track thermochronology. J. Geophys. Res. 107, B12, 2333, doi:10.1029/2001JB000745.

Bumby, A.J., Guiraud, R., 2005. The geodynamic setting of the Phanerozoic basins of Africa. J. Afr. Earth Sci. 43, 1–12.

Burke, K., 1996. The African Plate. South Afr. J. Geol. 99, 341–409.

Burke, K., Gunnell, Y., 2008. The African erosion surface: a continental-scale synthesis of geomorphology, tectonics, and environmental change over the past 180 million years,. Geol Soc Am Mem 201, 72.

Butt, C.R.M., Lintern, M.J., Anand, R.R., 2000. Evolution of regoliths and landscapes in deeply weathered terrain — implications for geochemical exploration. Ore Geol. Rev. 16, 167–183. https://doi.org/10.1016/S0169-1368(99)00029-3

Cande, S.C., LaBrecque, J.L., Haxby, W.F., 1988. Plate kinematics of the South Atlantic: Chron C34 to present. J. Geophys. Res. 93, 13479–13492.

Cockburn, H.A.P., Brown, R.W., Summerfield, M.A., Seidl, M.A., 2000. Quantifying passive margin denudation and landscape development using a combined fission-track thermochronology and cosmogenic isotope analysis approach. Earth Planet. Sci. Lett. 179, 429–435. https://doi.org/10.1016/s0012-821x(00)00144-8

Cockburn, H.A.P., Seidl, M.A., Summerfield, M.A., 1999. Quantifying denudation rates on inselbergs in the central Namib Desert using in situ-produced cosmogenic 10 Be and 26 Al. Geology 27, 399–402.

Cooper, A.F., 1988. Geology of Dicker Willem, a subvolcanic carbonatite complex in South-West Namibia. Commun. Geol. Surv. SW Afr. 4, 3–12.

Cox, K.G., 1989. The role of mantle plumes in the development of continental drainage patterns. Nature 342, 873–877.

Dauteuil, O., Bessin, P., Guillocheau, F., 2015. Cenozoic growth of the southern Africa landscape around the Orange Valley: a planation record of deformation and climate changes. Geomorphology 233, 5–19.

Dauteuil, O., Bouffette, J., Toteu, F.S., 2009. Visages du continent africain. CCGM, Paris, 48p.

Dauteuil, O., Deschamps, F., Bourgeois, O., Mocquet, A., Guillocheau, F., 2013a. Post-breakup evolution and palaeotopography of the North Namibian Margin during the Meso-Cenozoic. Tectonophysics 589, 103–115.

Dauteuil, O., Picart, C., Guillocheau, F., Pickford, M., Senut, B., 2018. Cenozoic deformation and geomorphic evolution of the Sperrgebiet area (Southern Namibia). Commun. Geol. Surv. Namib. 18, 1–18.

Dauteuil, O., Rouby, D., Braun, J., Guillocheau, F., Deschamps, F., 2013b. Post-breakup evolution of the margin of Namibia: constraints from numerical approach. Tectonophysics

604, 122–138.

de Wit, M., 2007. The Kalahari Epeirogeny and climate change: differentiating cause and effect from core to space. South Afr. J. Geol. 110, 367–392.

Doucoure, C.M., de Wit, M.J., 2003. Old inherited origin for the present near-bimodal topography of Africa. J. Afr. Earth Sci. 36, 371–388.

Dupont, L., Donner, B., Vidal, L. , Pérez, E., WeferLinking, G., 2005. Desert evolution and coastal upwelling: Pliocene climate change in Namibia. Geology 33, 461-464.

Fairhead, J.D., Binks, R.M., 1991. Differential opening of the Central and South Atlantic Oceans and the opening of the West African rift system. Tectonophysics 187, 191–203.

Fernàndez, M., Afonsoa, J.C., Ranalli, G., 2010. The deep lithospheric structure of the Namibian volcanic margin. Tectonophysics, 481, 68-81.

Flament, N., Gurnis, M., Williams, S., Seton, M., Skogseid, J., Heine, C., Dietmar Müller, R., 2014. Topographic asymmetry of the South Atlantic from global models of mantle flow and lithospheric stretching. Earth Planet. Sci. Lett. 387, 107–119. https://doi.org/10.1016/j.epsl.2013.11.017

Fleming, A., Summerfield, M.A., Stone, J.O., Fifield, L.K., Cresswell, R.G., 1999. Denudation rates of the southern Drakenberg escarpement, SE Africa, derived from in-situ-produced cosmogenic 36Cl: initial results. J. Geol. Soc. 156, 209–212.

Forte, A.M., Quéré, S., Moucha, R., Simmons, N.A., Grand, S.P., Mitrovica, J.X., Rowley, D.B., 2011. Joint seismic, geodynamic-mineral physical modelling of African geodynamics: A reconciliation of deep-mantle convection with surface geophysical constraints. Earth Planet. Sci. Lett. 295, 329–341.

Gallagher, K., Brown, R., 1999a. Denudation and uplift at passive margins: the record on the Atlantic Margin of southern Africa. Philos. Trans. R. Soc. Lond. A 357, 835–859.

Gallagher, K., Brown, R., 1999b. The oil and gas habitats of South Atlantic, in: Cameron, N.R., Bate, R.H., Clure, V.S. (Eds.), The Mesozoic Denudation History of the Atlantic Margins of Southern Africa and Southeast Brazil and the Relationship to Offshore Sedimentation. Geol. Soc. Sp. Public., London, pp. 41–53.

Gallagher, K., Brown, R., Johnson, C., 1998. Fission track analysis and its applications to geological problems. Annu. Rev. Earth Planet. Sci. 26, 519–572.

Geach, M.R., Stokes, M., Telfer, M.W., Mather, A.E., Fyfe, R.M., Lewin, S., 2014.The application of geospatial interpolation methods in the reconstruction of Quaternary landform records. Geomorphology, 216, 234-246

Genis, G., 1990. 2618 Keetmanshoop. Geological series.

Gilchrist, A.R., Summerfield, M.A., 1991. Denudation, isostasy and landscape evolution. Earth Surf. Process. Landf. 16, 555–562. https://doi.org/10.1002/esp.3290160607

Gilchrist,A. R., Summerfield, M. A., Cockburn, H. A. P., 1994. Landscape dissection, isostatic uplift, and the morphologic development of orogens. Geology, 22, 963-966.

Goudie, A., Viles, H., 2015. Calcretes: The Kamberg Calcrete Formation and the Karpencliff Conglomerate, in: Landscapes and Landforms of Namibia, World Geomorphological Landscapes. Springer, Dordrecht, pp. 111–114. https://doi.org/10.1007/978-94-017-8020-9_16

Goudie, A.S., 2005. The drainage of Africa since the Cretaceous. Geomorphology 67, 437–456.

Green, P.F., Japsen, P., Chalmers, J.A., Bonow, J.M., Duddy, I.R., 2018. Post-breakup burial and exhumation of passive continental margins: Seven propositions to inform geodynamic models. Rift. Passive Margins 53, 58–81. https://doi.org/10.1016/j.gr.2017.03.007

Gresse, P.G., Germs, G.J.B., 1993. The Nama foreland basin: sedimentation, major unconformity bounded sequences and multisided active margin advance. Precambrian Res. 63, 247–272. https://doi.org/10.1016/0301-9268(93)90036-2

Guillocheau, F., Chelalou, R., Linol, B., Dauteuil, O., Robin, C., Mvondo, F., Callec, Y., Colin, J.P., 2014. Cenozoic Landscape evolution in and around the Congo Basin: Constraints from sediments and planation surfaces, in: M.J. de Wit, F.G., M.C.J. de Wit, Guillocheau, F., De Wit, M.C.J. (Eds.), The Geology and Resource Potential of the Congo Basin. Springer-Verlag, Berlin, pp. 271–313.

Guillocheau, F., Simon, B., Baby, G., Bessin, P., Robin, C., Dauteuil, O., 2018. Planation surfaces as a record of mantle dynamics: The case example of Africa. Gondwana Res., Rifting to Passive Margins 53, 82–98. https://doi.org/10.1016/j.gr.2017.05.015

Gunnell, Y., Fleitout, L., 1998. Shoulder uplift of the Western Ghats passive margin, India: a denudational model. Earth Surf. Process. Landf. 23, 391–404. https://doi.org/10.1002/(SICI)1096-9837(199805)23:5<391::AID-ESP853>3.0.CO;2-5

Haddon, I.G., McCarthy, T.S., 2005. The Mesozoic-Cenozoic interior sag basins of Central Africa: The Late-Cretaceous-Cenozoic Kalahari and Okavango basins. J. Afr. Earth Sci. 43, 316–333. https://doi.org/10.1016/j.jafrearsci.2005.07.008

Hirsch, K.K., Scheck-Wenderoth, M., van Wees, J.-D., Kuhlmann, G., Paton, D.A., 2010. Tectonic subsidence history and thermal evolution of the Orange Basin. Mar. Pet. Geol. 27, 565–584.

Japsen, P., Chalmers, J.A., Green, P.F., Bonow, J.M., 2012. Elevated, passive continental margins: Not rift shoulders, but expressions of episodic, post-rift burial and exhumation. Glob. Planet. Change, Coupled deep Earth and surface processes in System Earth: monitoring, reconstruction and process modeling 90–91, 73–86. https://doi.org/10.1016/j.gloplacha.2011.05.004

Jourdan, F., Féraud, G., Bertrand, H., Kampunzu, A.B., Tsoho, G., Watkeys, M.K., Le Gall, B., 2005. Karoo large igneous province: Brevity, origin, and relation to mass extinction questioned by new 40Ar/39Ar age data. Geology 33, 745–748.

Jung, G., Prange, M., Schulz, M., 2014. Uplift of Africa as a potential cause for Neogene intensification of the Benguela upwelling system. Nature Geoscience, 7, 741–747

Kounov, A., Viola, G., de Wit, M.J., Andreoli, M., 2008. A Mid Cretaceous paleo-Karoo River valley across the Knersvlakte plain (northwestern coast of South Africa): Evidence from apatite fission-track analysis. South Afr. J. Geol. 111, 409-420. https://doi.org/10.2113/gssajg.111.4.409.

Kounov, A., Viola, G., de Wit, M.J., Andreoli,M.A.G., 2009. Denudation along the Atlantic passive margin: new insights from apatite fission-track analysis on the western coast of South Africa. Geol. Soc., London, Special Publications, 324, 287-306, https://doi-org.insu.bib.cnrs.fr/10.1144/SP324.19.

Kounov, A., Niedermann, S., de Wit, M.J., Viola, G., Andreoli, M., Erzinger, J., 2007.

Present denudation rates at selected sections of the South African escarpment and the elevated continental interior based on cosmogenic 3He and 21Ne. South Afr. J. Geol. 110, 235–248. https://doi.org/10.2113/gssajg.110.2-3.235

Kounov, A., Viola, G., Dunkl, I., Frimmel, H.E., 2013. Southern African perspectives on the long-term morpho-tectonic evolution of cratonic interiors. Tectonophysics 601, 177–191.

Le Breton, E., Cobbold, P.R., Dauteuil, O., Lewis, G., 2012. Variations in amount and direction of seafloor spreading along the northeast Atlantic Ocean and resulting deformation of the continental margin of northwest Europe. Tectonics 31, TC5006. https://doi.org/10.1029/2011TC003087

Leroy, M., Dauteuil, O., Cobbold, P., 2004. Compression of passive margins: controls from oceanic lithosphere rheology. Geophys. J. Int. 159, 400–411.

Linol, B., de Wit, M.J., Guillocheau, F., Robin, C., 2014. Multiphase Phanerozoic subsidence and uplift history recorded in the Congo Basin - A complex successor basin., in: de Wit, M.J., Guillocheau, F., de Wit, M.C.J., Guillocheau, F. (Eds.), Geology and Resource Potential of the Congo Basin. Springer-Verlag, Berlin, pp. 213–227.

Lock, B.E., 1973. Tertiary limestones at Needs Camp, near East London. Trans. Geol. Soc. South Afr. 76, 1–5.

Lorenz, V., Stachel, T., Kurszlaukis, S., Stanistreet, I.G., 2000. Volcanology of the Gross Brukkaros Field, South Namibia. Commun. Geol. Surv. Namib. 12, 347–352.

Luft, F.F., Luft, J.J.L., Chemale, J.F., Lelarge, M.L.M.V., Ávila, J.N., 2005. Post-Gondwana break-up record constraints from apatite fission track thermochronology in NW Namibia. Radiat. Meas. 39, 675–679. https://doi.org/10.1016/j.radmeas.2004.08.010

Marsh, J.S., 2010. The geochemistry and evolution of Palaeogene phonolites, central Namibia. Lithos 117, 149–160.

Marsh, J.S., Milner, S.C., 2007. Stratigraphic correlation of the Awahab and Tafelberg Formations, Etendeka Group, Namibia, and location of an eruptive site for flood basalt volcanism. J. Afr. Earth Sci. 48, 329–340.

Miller, K.G., Moutain, G.S., Wright, J.D., Browing, J.V., 2011. A 180-Million-Year Record of Sea Level and Ice Volume Variations from Continental Margin and Deep-Sea Isotopic

Records. Oceanography 24, 40–53.

Miller, R.M., Becker, T., Geological Survey of Namibia, 2008. The geology of Namibia. Ministry of Mines and Energy, Geological Survey, Windhoek, Namibia.

Moulin, M., 2003. Etude géologique et géophysique dees marges continentales passives : exemples du Zaïre et de l'Angola (PhD Thesis). Université de Bretagne Occidentale, Brest, France.

Müller, R.D., Sdoria, M., Gaina, C., 2008. Age, spreading rates and spreading symmetry of the world's ocean crust, Geochem. Geophys. Geosyst., 9, Q04006, doi:10.1029/2007GC001743. Geochem Geophys Geosyst 9, Q04006. https://doi.org/0.1029/2007GC001743.

Mvondo, F., Dauteuil, O., Guillocheau, F., 2011. The Fish River canyon (Southern Namibia): A record of Cenozoic mantle dynamics? Comptes Rendus Geosci. 343, 478–485.

Mvondo Owono, F., Ntamak-Nida, M.-J., Dauteuil, O., Guillocheau, F., Njom, B., 2016. Morphology and long-term landscape evolution of the South African plateau in South Namibia. Catena 142, 47–65. https://doi.org/10.1016/j.catena.2016.02.012

Nguno, A.K., 2004. Kimberlite indicator of the Gibeon Kimberlite Province (GKP), southern Namibia: Their character and distribution in kimberlite intrusions and fluvial sediments. Commun. Geol. Surv. Namib. 13, 33–42.

Nyblade, A.A., Sleep, N.H., 2003. Long lasting epeirogenic uplift mantle plumes and the origin of the Southern African Plateau. Geochem. Geophys. Geosystems 4, 1105, doi 10.1029/2003GC0000573.

Olivet, J.-L., Bonnin, J., Beuzart, P., Auzende, J.-M., 1984. Cinématique de l'Atlantique Nord et Central.— Rapp. Sci. Tech. C.N.E.X.O., v. 54, 108 p., Rapp. Sci. Tech. C.N.E.X.O.

Owen-Smith, T.M., Ganerød, M., van Hinsbergen, D.J.J., Gaina, C., Ashwal, L.D., Torsvik, T.H., 2017. Testing Early Cretaceous Africa–South America fits with new palaeomagnetic data from the Etendeka Magmatic Province (Namibia). Tectonophysics. https://doi.org/10.1016/j.tecto.2017.11.010

Parrish, J.T., Ziegler, A.M., Scotese, C.R., 1982. Rainfall patterns and the distribution of coals and evaporites in the Mesozoic and Cenozoic. Palaeogeogr. Palaeoclimatol. Palaeoecol., Paleogeography and Climate 40, 67–101. https://doi.org/10.1016/0031-0182(82)90085-2

Partridge, T.C., Maud, R.R., 2000. The Cenozoic of Southern Africa, 40th ed, Oxford Monographs on Geology and Geophysics. University Press, Oxford.

Partridge, T.C., Maud, R.R., 1987. Geomorphic evolution of Southern Africa since the Mesozoic. South Afr. J. Geol. 90, 179–208.

Pastier, A.-M., Dauteuil, O., Murray-Hudson, M., Moreau, F., Walpersdorf, A., Makati, K., 2017. Is the Okavango Delta the terminus of the East African Rift System? Towards a new geodynamic model: Geodetic study and geophysical review. Tectonophysics 712–713, 469–481. https://doi.org/10.1016/j.tecto.2017.05.035

Pickford, M., 2016. Cenozoic Geology of the Northern Sperrgebiet, Namibia,. Commun. Geol. Surv. Namib. 10–104.

Pickford, M., Eisenmann, V., Senut, B., 1999. Timing of landscape development and calcrete genesis in northern Namaqualand, South Africa. South Afr. J. Sci. 95, 357–359.

Pickford, M., Senut, B., 2003. Miocène Paleobiology of the Orange River Valley, Namibia. Memoire Geol. Surv. Namib. 19, 1-22.

Pickford, M., Senut, B., 1999. Geology and palaeobiology of the Namib desert Southwest Africa. Geol. Surv. Namib. Mem. 18, 155 p.

Pickford, M., Senut, B., Mocke, H., Mourer-Chauviré, C., Rage, J.-C., Mein, P., 2014. Eocene aridity in southwestern Africa: timing of onset and biological consequences. Trans. R. Soc. South Afr. 69, 139–144. https://doi.org/10.1080/0035919X.2014.933452

Pysklywec, R.N., Mitrovica, J.X., 1999. The role of subduction-induced subsidence in the evolution of the Karoo Basin. J. Geol. 107, 155–164.

Raab, M.J., 2002. Late Cretaceous reactivation of major crustal shear zones in northern Namibia; constraints from apatite fission track analysis. Tectonophysics 349, 75–92.

Raab, M.J., Brown, R.W., Gallagher, K., Carter, A., Weber, K., 2002. Late Cretaceous reactivation of major crustal shear zones in northern Namibia: constraints from apatite fission track analysis. Tectonophysics 349, 75–92.

Rouby, D., Braun, J., Robin, C., Dauteuil, O., Deschamps, F., 2013. Long-term stratigraphic evolution of Atlantic-type passive margins: A numerical approach of interactions between surface processes, flexural isostasy and 3D thermal subsidence. Tectonophysics, 604, 83-103

Rovere, A., Raymo, M.E., Mitrovica, J.X., Hearty, P.J., O'Leary, M.J., Inglis, J.D., 2014. The Mid-Pliocene sea-level conundrum: Glacial isostasy, eustasy and dynamic topography. Earth Planet. Sci. Lett. 387, 27–33. https://doi.org/10.1016/j.epsl.2013.10.030

Salomon, E., Koehn, D., Passchier, C., Hackspacher, P.C., Glasmacher, U.A., 2015. Contrasting stress fields on correlating margins of the South Atlantic. Gondwana Res. 28, 1152–1167. https://doi.org/10.1016/j.gr.2014.09.006

Schmidt, K.-H., 1989. The significance of scarp retreat for cenozoic landform evolution on the Colorado Plateau, U.S.A. Earth Surf. Process. Landf. 14, 93–105. https://doi.org/10.1002/esp.3290140202

Schreiber, U.M., Becker, T., 1999. 2716 Ai-Ais. Geological map of Namibia.

Simmons, N.A., Forte, A.M., Grand, S.P., 2009. Joint seismic, geodynamic and mineral physical constraints on three-dimensional mantle heterogeneity: Implications for the relative importance of thermal versus compositional heterogeneity. Geophys. J. Int. 177, 1284–1304. https://doi.org/10.1111/j.1365-246X.2009.04133.x

Smith, A.G., 1982. Late Cenozoic uplift of stable continents in a reference frame fixed to South America Nature, 296, 400-404

Stanistreet, I.G., Charlesworth, E.G., 2001. Damaran basement-cored fold nappes incorporating pre-collisional basins, Kaoko Belt, Namibia, and controls on Mesozoic supercontinent break-up. South Afr. J. Geol. 104, 1–12.

Steckler, M.S., Omar, G.I., 1994. Controls on erosional retreat of the uplifted rift flanks at the Gulf of Suez and northern Red Sea. J. Geophys. Res. Solid Earth 99, 12159–12173. https://doi.org/10.1029/94JB00278

Stollhofen, H., Gerschutz, S., Stanistreet, I.G., Lorenz, V., 1998. Tectonic and volcanic controls on Early Jurassic rift-valley lake deposition during emplacement of Karoo flood basalts, southern Namibia. Palaeogeogr. Palaeoclimatol. Palaeoecol. 140, 185–215.

Tardy, Y., 1993. Pétrologie des latérites et des sols tropicaux. Masson, Paris, 459 p.

Tinker, J., de Wit, M., Brown, R., 2008a. Linking source and sink: Evaluating the balance between onshore erosion and offshore sediment accumulation since Gondwana break-up, South Africa. Tectonophysics 455, 94–103.

Tinker, J., de Wit, M., Brown, R., 2008b. Mesozoic exhumation of the southern Cape, South Africa, quantified using apatite fission track thermochronology. Tectonophysics 455, 77–93. https://doi.org/10.1016/j.tecto.2007.10.009

van der Beek, P., Summerfield, M., A., Braun, J., Brown, R., W., Fleming, A., 2002. Modeling postbreakup landscape development and denudational history across the southeast African (Drakensberg Escarpment) margin. J. Geophys. Res. 107, 2351, doi:10.1029/2001JB000744.

Wanke, H., Wanke, A., 2007. Lithostratigraphy of the Kalahari Group in northeastern Namibia. J. Afr. Earth Sci. 48, 314–328.

Ward, J.D., 1987. The Cenozoic succession in the Kuiseb Valley, central Namib Desert. Geol. Surv. South West Afr. Mem. 9, 124 p.

Watchman, A.L., Twidale, C.R., 2002. Relative and 'absolute' dating of land surfaces. Earth-Science Reviews, 58, 1-49

White, S., Stollhofen, H., Stanistreet, I.G., Lorenz, V., 2009. Pleistocene to Recent rejuvenation of the Hebron Fault, SW Namibia. Geol. Soc. Lond. Spec. Publ. 316, 293–317. https://doi.org/10.1144/SP316.18

Wildman, M., Brown, R., Beucher, R., Persano, C., Stuart, F., Gallagher, K., Schwanethal, J., Carter, A., 2016. The chronology and tectonic style of landscape evolution along the elevated Atlantic continental margin of South Africa resolved by joint apatite fission track and (U-Th-Sm)/He thermochronology. Tectonics 35, 2015TC004042. https://doi.org/10.1002/2015TC004042

Zerfass, H., Chemale F., ErnestoLavina, E., 2005. Tectonic Control of the Triassic Santa Maria Supersequence of the Paraná Basin, Southernmost Brazil, and its Correlation to the Waterberg Basin, Namibia. Gondwana Research, 8, 163-176

Figure caption:

Figure 1: Topographic map of the study area with the main scarp (white line) and the different geomorphic domains: Damara, inner, coastal, Orange. The upper right insert displays the location of the study area.

Figure 2: Pictures of the main geomorphic features: 2a) unconformity (white line) between the Nama Group (NG) and the Namaqualand Metamorphic Complex (NMCpl) in the Fish River Canyon, 2b) high inselbergs to the south of Windhoek, 2c) the slightly weathered phonolites of Aris, 2d) weathered Late Karoo basalts to the south of Mariental, 2e) lateritic profile in the Sperrgebiet (Chocolateberg), 2f) landscape in the Sperrgebiet showing the filled paleovalley incised into surface S7. The planation surfaces are annotated on the various pictures.

Figure 3: Planation surfaces as markers of short and long wavelength deformations. Figure 3a presents the five types of relative chronologies between faults and planation surfaces. Note that a scarp is not systematically symptomatic of a fault. Figure 3b displays how the planation surfaces accommodate long wavelength deformation. Three cases: global uplift, local bending and tilting. The histograms in the right column show the elevation distribution for each case, the yellow bars represent the reference distribution of normal altitudes of a planation surface (top frame) while the purple bars indicate the elevation distribution after deformation. Note that the distribution width increases when bending and tilting occur compared to the typical distribution of a planation surface (upper right).

Figure 4: Relative chronology between planation surfaces and magmatic events. A) The magmatic massif intrudes the planation surface: planation occurred before the magmatic event. B) The planation surface affects a preexisting magmatic massif that is eroded: planation occurs after the magmatic event.

Figure 5: Map of the planation surfaces. The black lines show the location of the cross-sections given in Figure 7. The lower left insert displays the elevation distribution for each surface.

Figure 6: Elevation of the unconformity between the Nama Group and the Namaqualand Metamorphic Complex. The elevations were estimated from outcrops, remote sensing images, DEM and synthetic cross-sections given in Figure 7. The Delaunay triangles method coupled with the nearest-neighbor interpolation was used to generate the elevation map. The local dips (blue symbols) were estimated from the cross-sections and from the map. The white dashed line delimits the known extent of the Nama Basin (Gresse and Germs, 1993).

Figure 7: Geological cross sections; 7a: N-S sections located to the east of the coastal plain and inland, 7b: E-W sections. The locations are depicted in Figure 5. The tables below each section report the average slope of the surfaces in each domain. Note the two sets of surfaces (S4-S5 and S6-S7-S8) on the western section (7a) and the change in surface organization from north to south by comparing the northern and southern sections (7b).

Figure 8: Stratigraphic section and detailed pictures of the alluvial delta located to the east of Mariental (24.6445°S, 18.0219°E). This alluvial delta overlies weathered Karoo basalts (lower picture) and surface S3. It is composed of two main terrigenous units: the lower conglomerate with weathered basalt clasts and the upper one without basalt clasts.

Figure 9: Compilation of the Cenozoic events including dated markers (magmatic events and deposits), planation surfaces, deformation event and climates. See the text for references regarding magmatism, deposits, sea level and climate changes.

Figure 10: Map of the medium-to-long wavelength deformation deduced from the organization of the planation surfaces. See the text for detailed explanations. The Kalahari Sands are in yellow and the white line displays the current location of the escarpment. Note that the maximum of uplift shows the bulge as being roughly parallel to the coast and that the current scarp follows the greatest uplift.

Figure 11: Morphotectonic evolution of the Namibian plateau and margin during the Cenozoic in five steps. Paleocene weathering and Oligocene bulging drive the geomorphic evolution.

Tables

Surface	Description	Driving process	Climate
Peneplain:	Gently undulating surface, almost featureless. 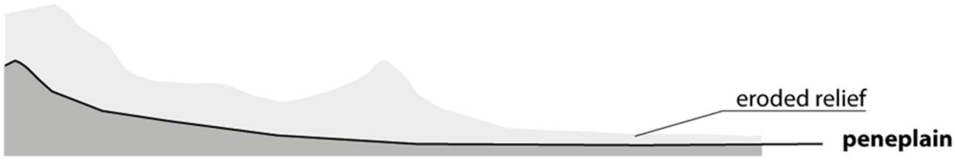 	Fluvial erosion	Very humid, moderate temperature
Pediplain:	The surface forms via a set of pediments fashioned during slope retreat. They may have a thin veneer of sediment. 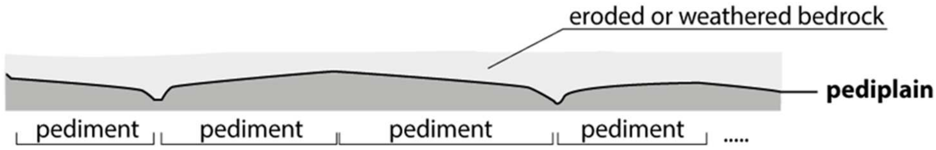 	Weathering and rare flash floods	Arid to semi-arid, hot
Etchplain:	Residual surface exposing an old weathered front. Residual reliefs (inselberg) may remain. 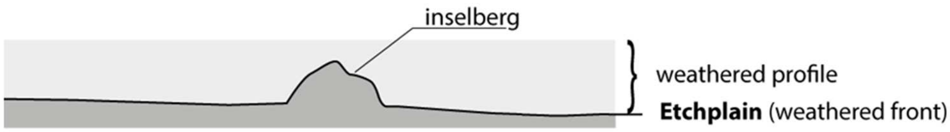 	Mechanical ablation of the weathering profile	Humid, temperate
Wavecut platform:	Flat area often found at the base of a sea cliff or along the shoreline of a lake or sea.  	Ablation by waves	Independent (?)

Table 1: Genetic planation surfaces of the inland domains (Dauteuil et al., 2015; Guillocheau et al., 2018).

Surface name	Type of basement	Landform shape	Relationships with other markers	Type of planation surfaces
S0	Meso-Proterozoic basement of the Damara Belt in the Windhoek area.	Discontinuous, elevated summits.	Higher surface.	Undetermined.
S1	Meso-Proterozoic basement of the Damara Belt in the Windhoek area.	Continuous elevated surface.	Degradation of S0.	Peneplain with southeast drainage.
S2	Meso-Proterozoic basement of the Damara Belt.	Large valleys opening westward.		Pediplain with southwestward drainage.
S3	On Proterozoic basement and Karoo basalts.	- Inselbergs and laterites. - Slopes decreasing southwards.	- Affects Rehobot phonolites.	Stripped etchplain.
S4	Only on Nama sediment.	Largely continuous with gentle slope southwards.	- Base of the delta at Mariental. - Offset by faults.	Peneplain driven by lithology with southward drainage.
S5	On Nama sediments and on Proterozoic basement.	- Largely continuous, degraded in the south - Bending	- Affects the delta at Mariental. - Offset by faults.	Peneplain driven by lithology with a base level associated with the Orange River.
S6	On Meso-Proterozoic basement and Neo-Proterozoic sediments.	Pedivalleys with low relief between them.	- Covered by Kalahari calcrete.	Pediplain with drainage flowing toward the east and southeast.
S7	Band close to the shoreline largely expanded in the north.	Seaward locally associated with marine erosion.	Below the recent dunes of the Namib Desert.	Peneplain to wavecut platform with a marine base level.
S8	On the Meso-Proterozoic basement and in the Gariep domain.	Pedivalleys and pediments located in the coastal domain, in the Orange valley and in recent rivers.	Incised by the present-day river.	Coastal to pediplain with drainage flowing toward the south and west.

Table 2: Characteristics of the planation surface from upper/older to lower/younge

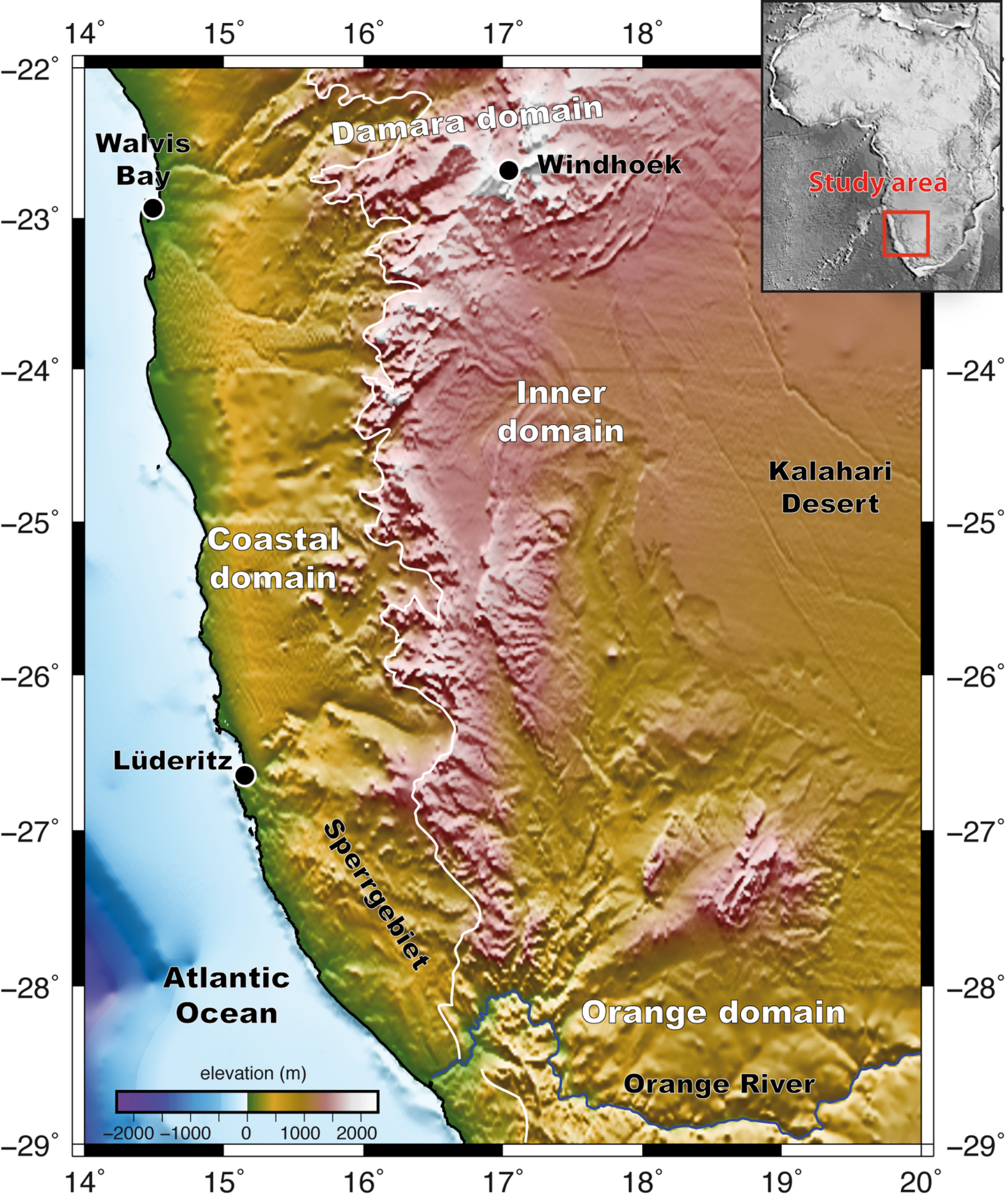

14°
15°
16°
17°
18°
19°
20°
−22°
−23°
−24°
−25°
−26°
−27°
−28°
−29°
Study area
Damara domain
Walvis Bay
Windhoek
Inner domain
Kalahari Desert
Coastal domain
Lüderitz
Sperrgebiet
Atlantic Ocean
Orange domain
Orange River
elevation (m)
−2000
−1000
0
1000
2000

Figure 1

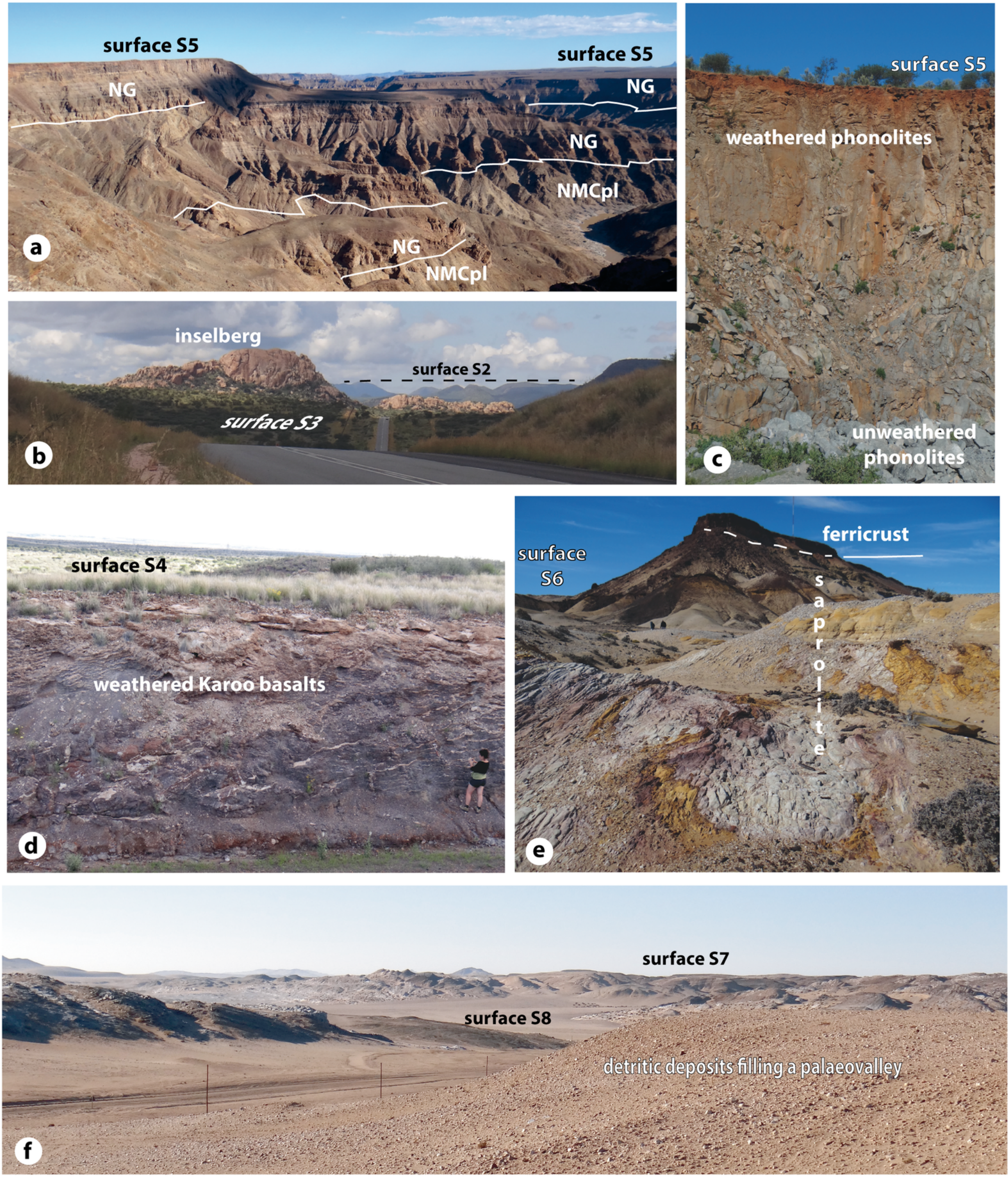
surface S5
surface S5
NG
NG
NG
NMCpl
NG
NMCpl
a
surface S5
weathered phonolites
unweathered phonolites
c
inselberg
surface S2
surface S3
b
surface S4
weathered Karoo basalts
d
surface S6
ferricrust
saprolite
e
surface S7
surface S8
detritic deposits filling a palaeovalley
f

Figure 2

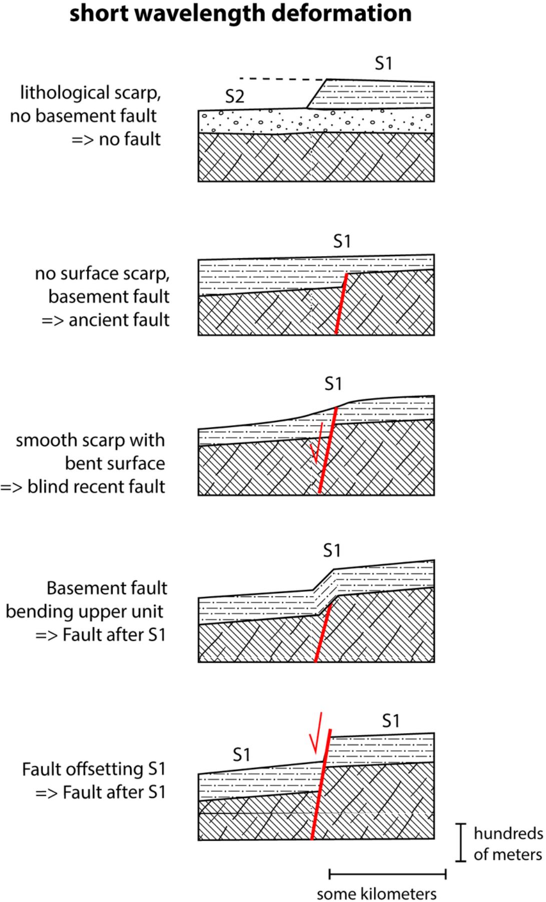

Figure 3a

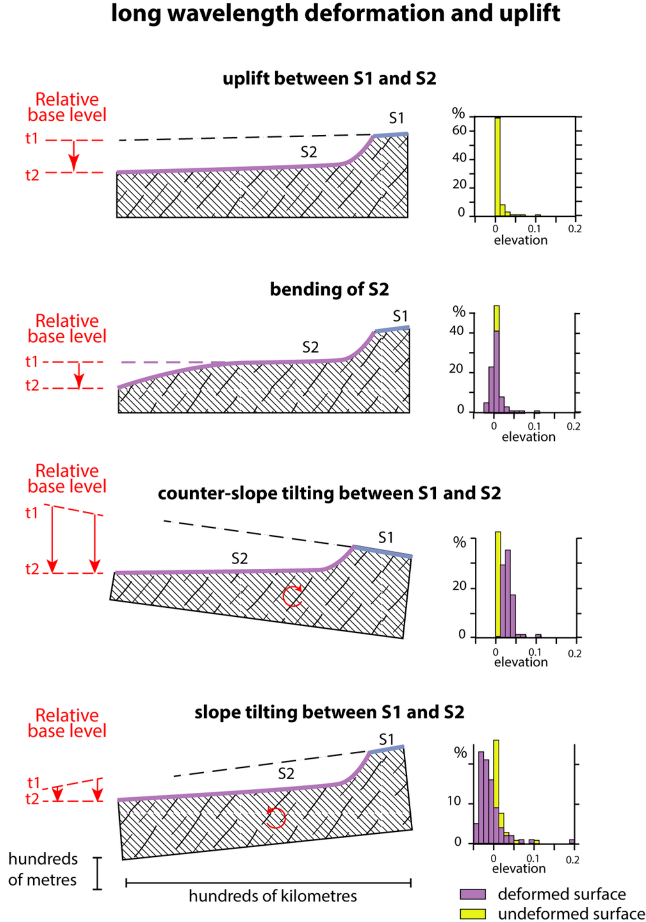

Figure 3b

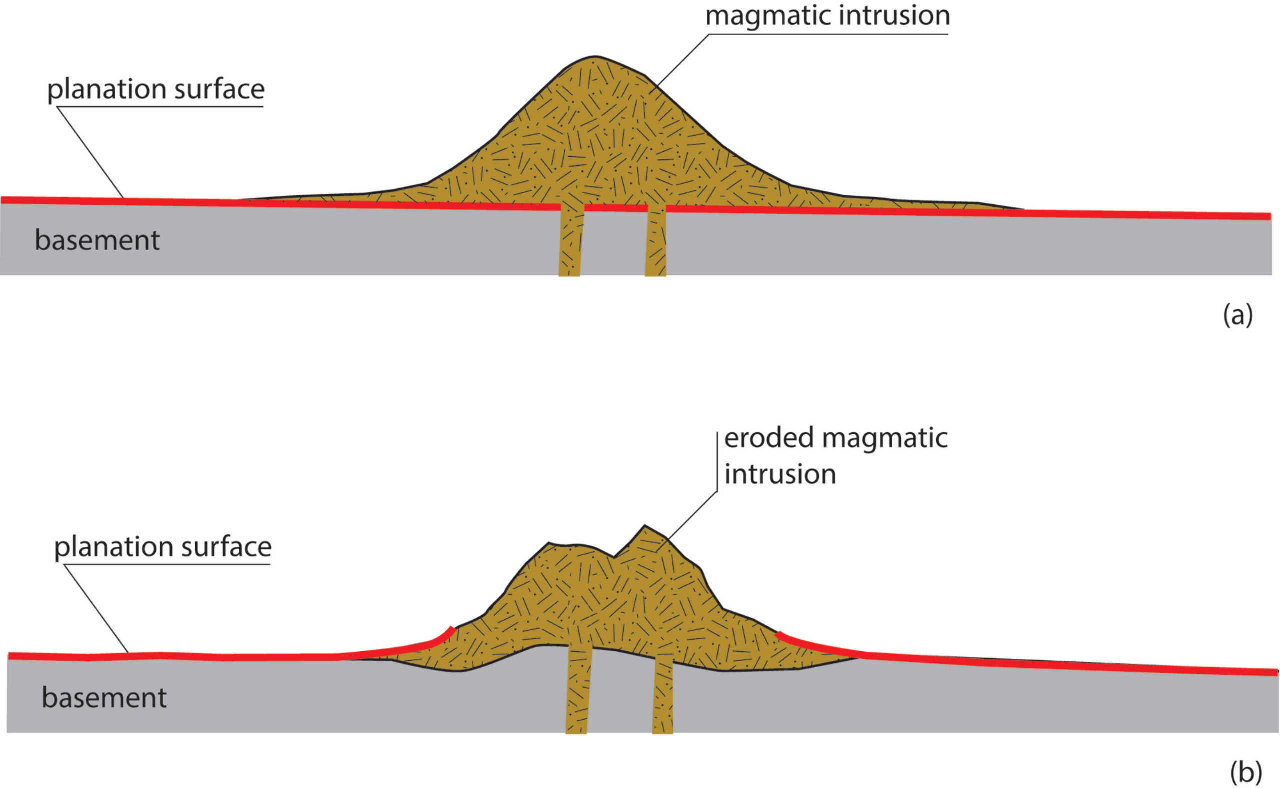
magmatic intrusion
planation surface
basement
(a)
eroded magmatic intrusion
planation surface
basement
(b)

Figure 4

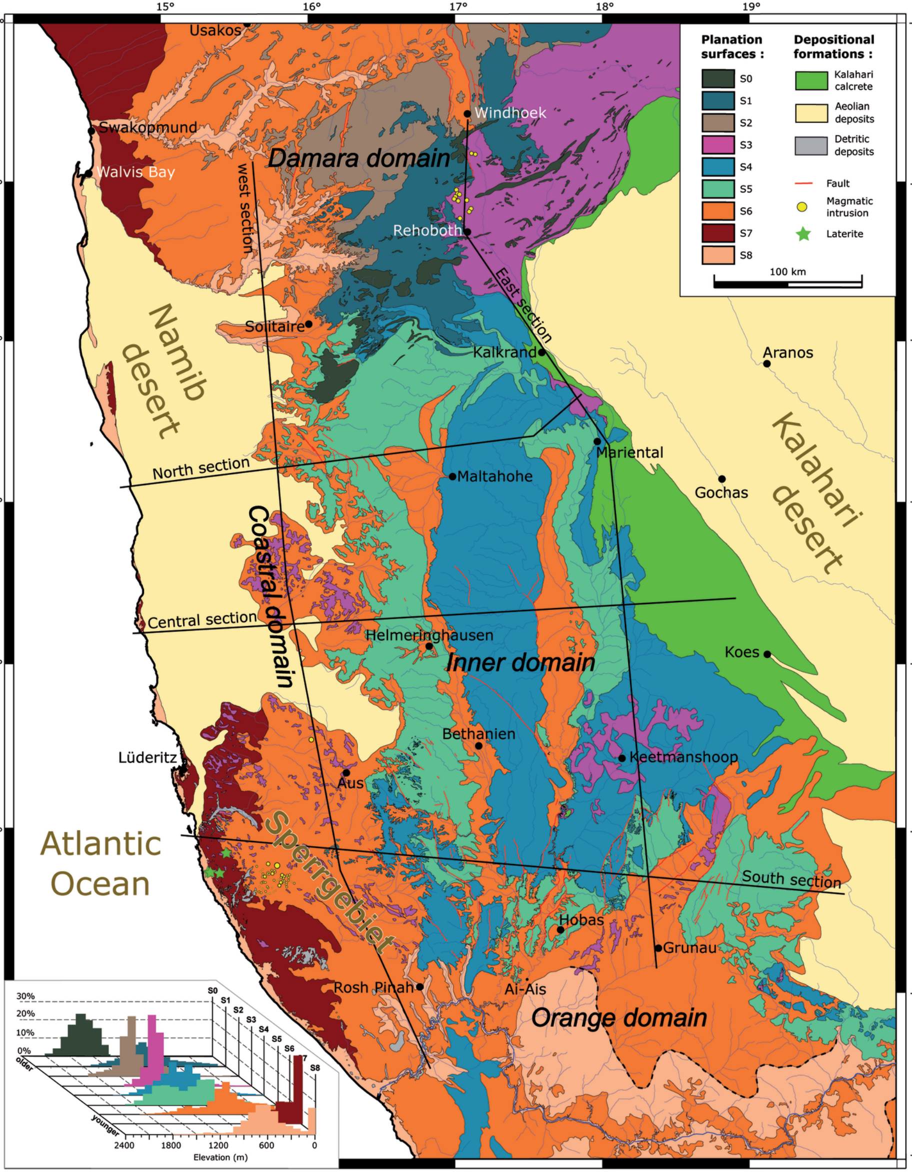

Planation surfaces :
S0
S1
S2
S3
S4
S5
S6
S7
S8
Depositional formations :
Kalahari calcrete
Aeolian deposits
Detritic deposits
Fault
Magmatic intrusion
Laterite
100 km
15°
16°
17°
18°
19°
-22°
-23°
-24°
-25°
-26°
-27°
-28°
-29°
Usakos
Swakopmund
Walvis Bay
Windhoek
Rehoboth
Damara domain
west section
East section
Solitaire
Kalkrand
Aranos
Namib desert
Kalahari desert
Mariental
Gochas
North section
Maltahohe
Coastral domain
Central section
Helmeringhausen
Inner domain
Koes
Bethanien
Lüderitz
Keetmanshoop
Aus
Atlantic Ocean
Sperrgebiet
South section
Hobas
Grunau
Rosh Pinah
Ai-Ais
Orange domain
30%
20%
10%
0%
older
younger
S0
S1
S2
S3
S4
S5
S6
S7
S8
2400
1800
1200
600
0
Elevation (m)

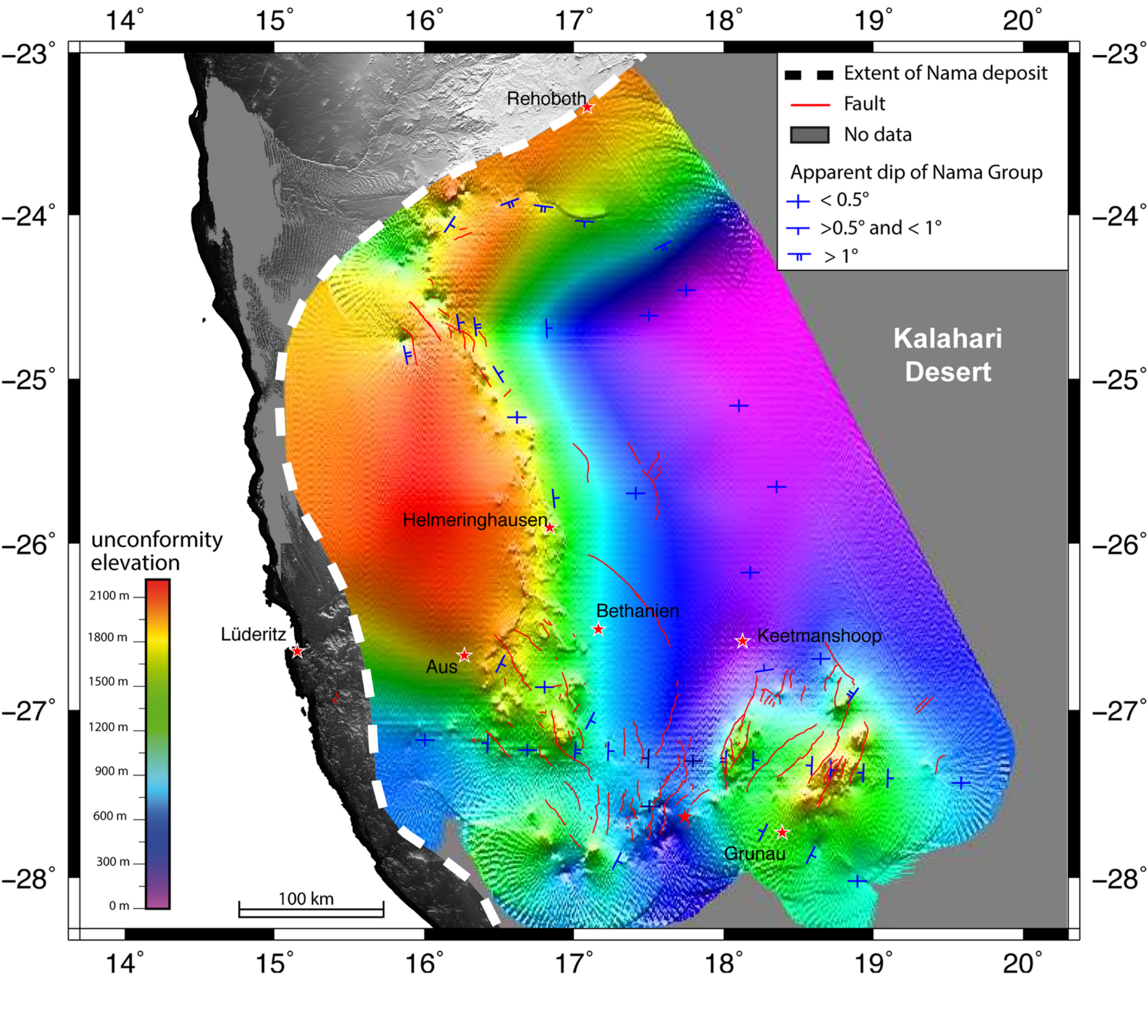

Extent of Nama deposit
Fault
No data
Apparent dip of Nama Group
< 0.5°
>0.5° and < 1°
> 1°
Kalahari Desert
Rehoboth
Helmeringhausen
Bethanien
Keetmanshoop
Lüderitz
Aus
Grunau
unconformity elevation
2100 m
1800 m
1500 m
1200 m
900 m
600 m
300 m
0 m
100 km
14°
15°
16°
17°
18°
19°
20°
-23°
-24°
-25°
-26°
-27°
-28°

Figure 6

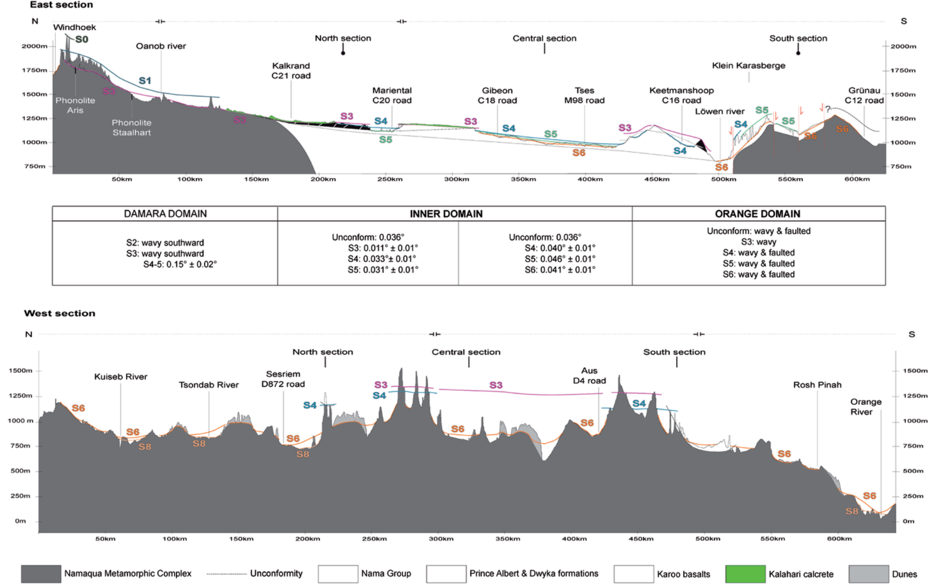

Figure 7a

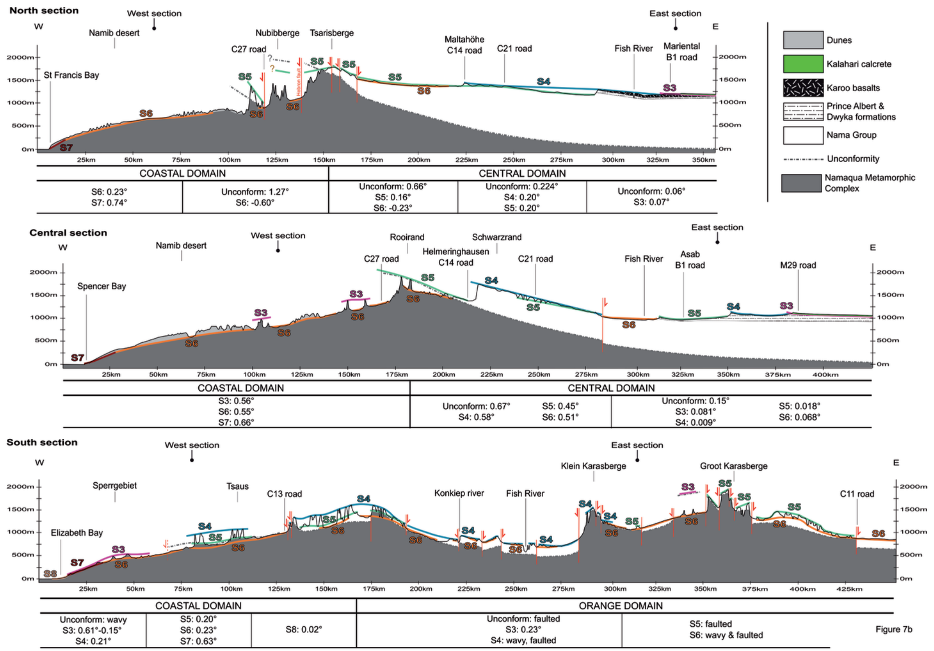

Figure 7b

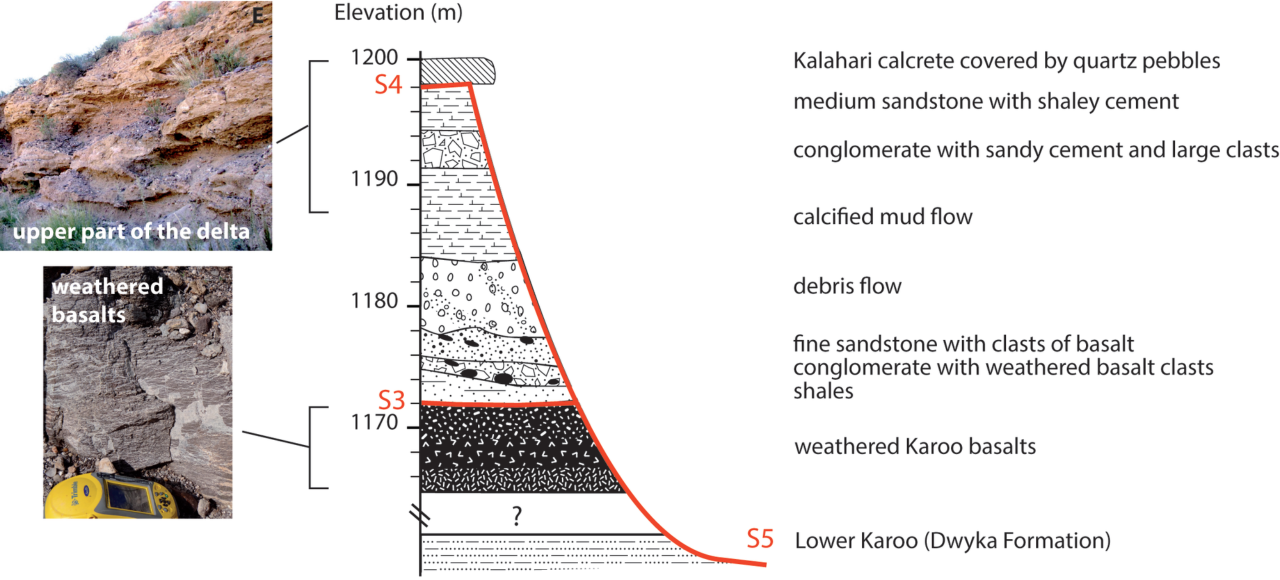
E
upper part of the delta
weathered basalts
Elevation (m)
1200
1190
1180
1170
S4
S3
S5
?
Kalahari calcrete covered by quartz pebbles
medium sandstone with shaley cement
conglomerate with sandy cement and large clasts
calcified mud flow
debris flow
fine sandstone with clasts of basalt
conglomerate with weathered basalt clasts
shales
weathered Karoo basalts
Lower Karoo (Dwyka Formation)

Figure 8

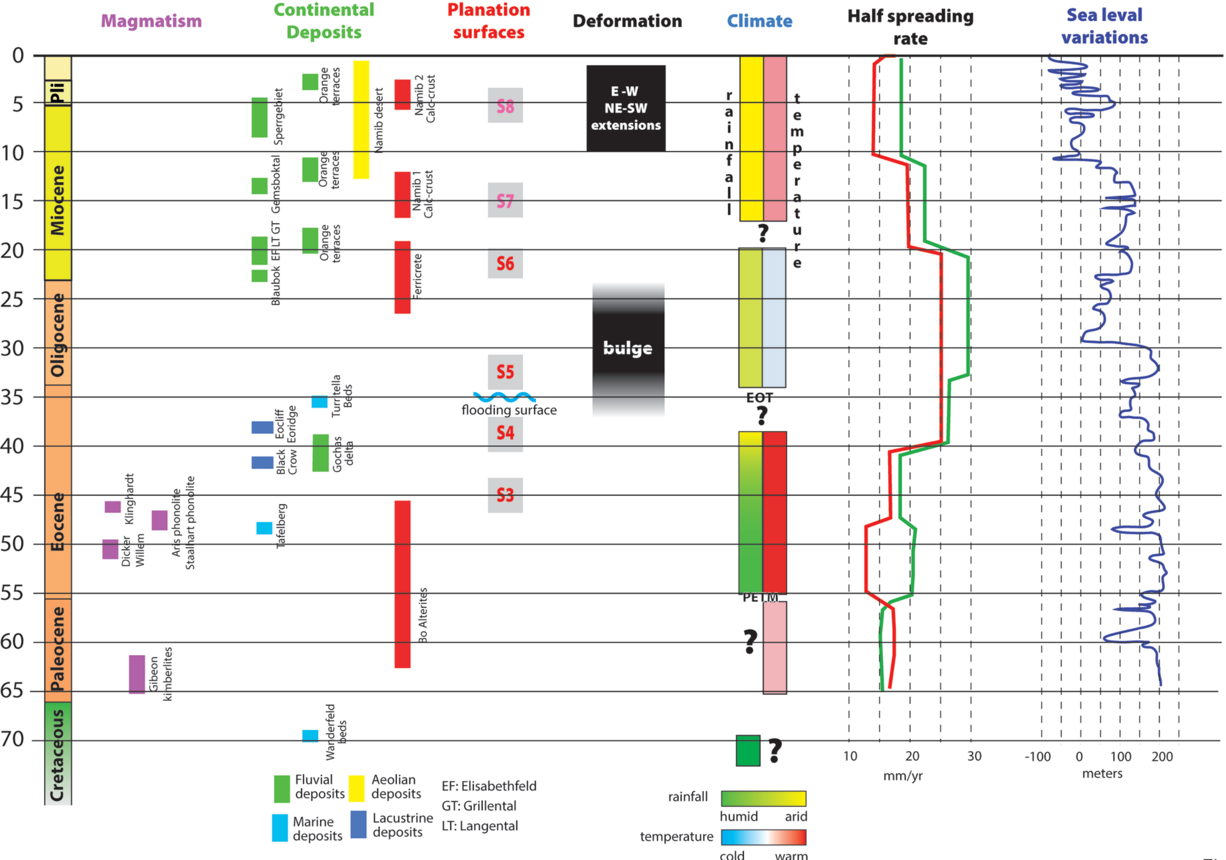
Magmatism
Continental Deposits
Planation surfaces
Deformation
Climate
Half spreading rate
Sea leval variations
0
5
10
15
20
25
30
35
40
45
50
55
60
65
70
Pli
Miocene
Oligocene
Eocene
Paleocene
Cretaceous
Klinghardt
Dicker Willem
Aris phonolite
Staalhart phonolite
Gibeon kimberlites
Sperrgebiet
Gemsboktal
Baubok EF LT GT
Orange terraces
Namib desert
Turritella Beds
Eocliff Eoridge
Black Crow
Gochas delta
Tafelberg
Wanderfeld beds
Namib 2 Calc-crust
Namib 1 Calc-crust
Ferricrete
Bo Alterites
S8
S7
S6
S5
flooding surface
S4
S3
E -W NE-SW extensions
bulge
rainfall
temperature
?
EOT
PETM
10
20
30
mm/yr
-100
0
100
200
meters
Fluvial deposits
Aeolian deposits
Marine deposits
Lacustrine deposits
EF: Elisabethfeld
GT: Grillental
LT: Langental
rainfall
humid
arid
temperature
cold
warm

Figure 9

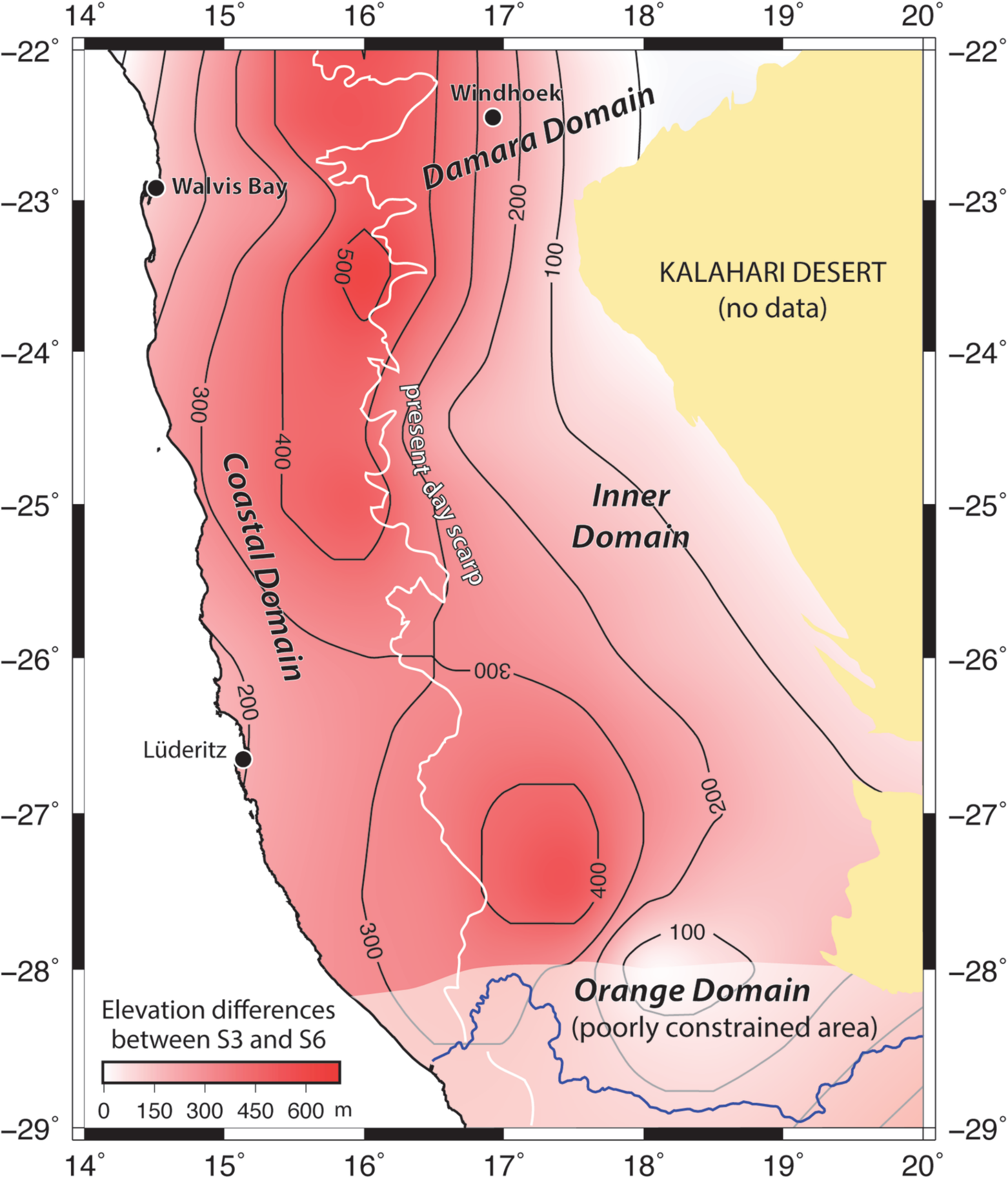

Windhoek
Damara Domain
Walvis Bay
KALAHARI DESERT
(no data)
present day scarp
Coastal Domain
Inner Domain
Lüderitz
Orange Domain
(poorly constrained area)
Elevation differences between S3 and S6
0 150 300 450 600 m
500
400
300
200
100

Figure 10

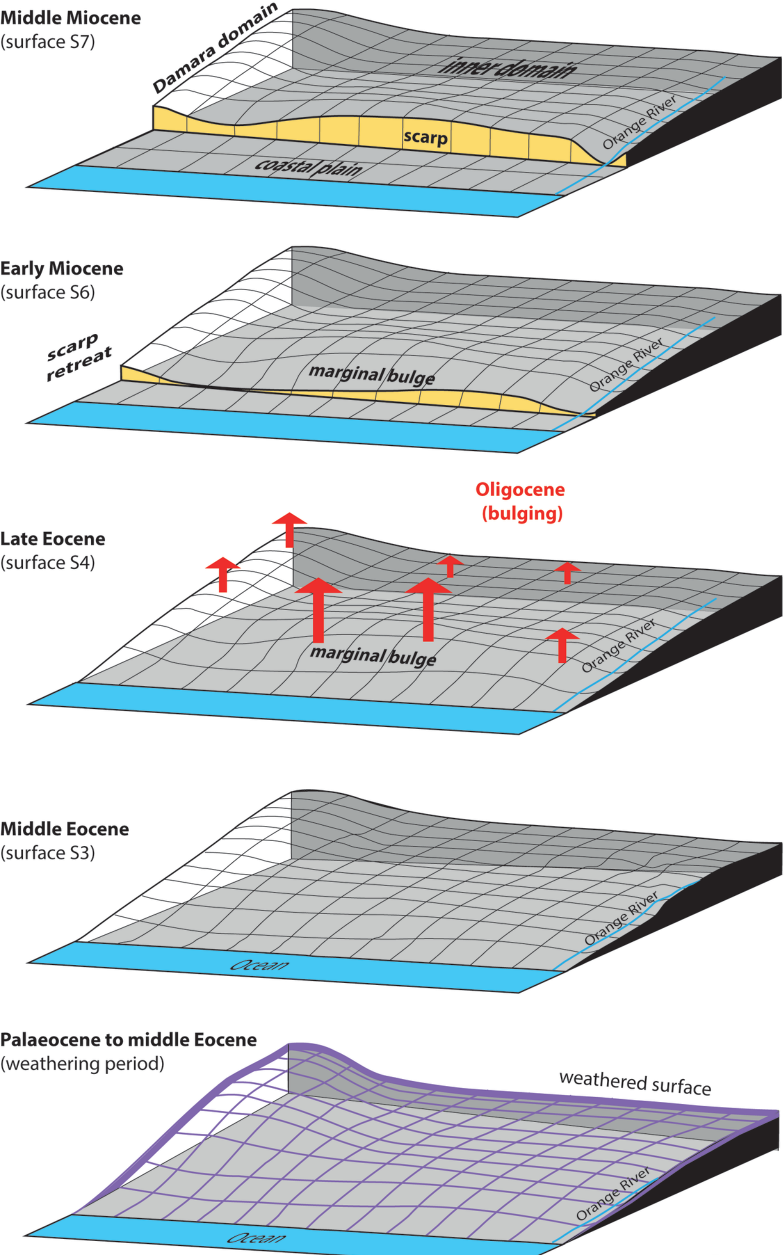
Middle Miocene
(surface S7)
Damara domain
inner domain
scarp
coastal plain
Orange River
Early Miocene
(surface S6)
scarp retreat
marginal bulge
Orange River
Oligocene
(bulging)
Late Eocene
(surface S4)
marginal bulge
Orange River
Middle Eocene
(surface S3)
Orange River
Ocean
Palaeocene to middle Eocene
(weathering period)
weathered surface
Orange River
Ocean

Figure 11

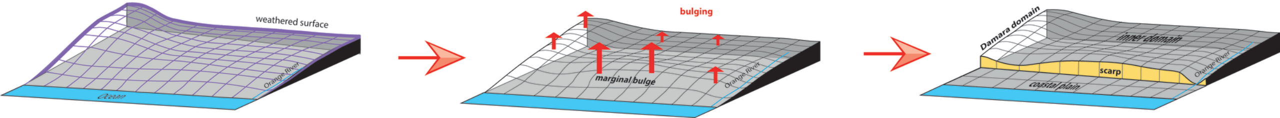
weathered surface
Orange River
Ocean
bulging
marginal bulge
Orange River
Damara domain
inner domain
scarp
Orange River
coastal plain